MOLECULAR AND CELLULAR BIOLOGY, Nov. 2008, p. 6757–6772 Vol. 28, No. 22
0270-7306/08/$08.00+0 doi:10.1128/MCB.00037-08

Drosophila Maternal *Hsp83* mRNA Destabilization Is Directed by Multiple SMAUG Recognition Elements in the Open Reading Frame▽†

Jennifer L. Semotok,[1,2] Hua Luo,[1,2] Ramona L. Cooperstock,[1,2] Angelo Karaiskakis,[1,2] Heli K. Vari,[3] Craig A. Smibert,[3] and Howard D. Lipshitz[1,2]*

Department of Molecular Genetics, University of Toronto, 1 King's College Circle, Toronto, Ontario M5S 1A8, Canada[1]; Program in Developmental and Stem Cell Biology, Research Institute, The Hospital for Sick Children, 101 College Street, Toronto, Ontario M5G 1L7, Canada[2]; and Department of Biochemistry, University of Toronto, 1 King's College Circle, Toronto, Ontario M5S 1A8, Canada[3]

Received 9 January 2008/Returned for modification 28 February 2008/Accepted 5 September 2008

SMAUG (SMG) is an RNA-binding protein that functions as a key component of a transcript degradation pathway that eliminates maternal mRNAs in the bulk cytoplasm of activated *Drosophila melanogaster* eggs. We previously showed that SMG destabilizes maternal *Hsp83* mRNA by recruiting the CCR4-NOT deadenylase to trigger decay; however, the *cis*-acting elements through which this was accomplished were unknown. Here we show that *Hsp83* transcript degradation is regulated by a major element, the *Hsp83* mRNA *i*nstability *e*lement (HIE), which maps to a 615-nucleotide region of the open reading frame (ORF). The HIE is sufficient for association of a transgenic mRNA with SMG protein as well as for SMG-dependent destabilization. Although the *Hsp83* mRNA is translated in the early embryo, we show that translation of the mRNA is not necessary for destabilization; indeed, the HIE functions even when located in an mRNA's 3′ untranslated region. The *Hsp83* mRNA contains eight predicted SMG recognition elements (SREs); all map to the ORF, and six reside within the HIE. Mutation of a single amino acid residue that is essential for SMG's interaction with SREs stabilizes endogenous *Hsp83* transcripts. Furthermore, simultaneous mutation of all eight predicted SREs also results in transcript stabilization. A plausible model is that the multiple, widely distributed SREs in the ORF enable some SMG molecules to remain bound to the mRNA despite ribosome transit through any individual SRE. Thus, SMG can recruit the CCR4-NOT deadenylase to trigger *Hsp83* mRNA degradation despite the fact that it is being translated.

During animal oogenesis and early embryogenesis, posttranscriptional gene regulation represents an essential mechanism for the control of gene expression. Mature oocytes and early embryos are transcriptionally quiescent and rely upon maternally supplied mRNAs deposited during oogenesis (5, 37). Often, multiple mechanisms of posttranscriptional control act coordinately to precisely regulate the spatial and temporal expression of proteins derived from these maternal mRNAs (23, 25).

In *Drosophila melanogaster*, the first 2½ hours of embryogenesis are programmed by maternal mRNAs (38). A surprisingly large fraction of the protein coding genome is present in this maternal transcript pool, with between one-half and two-thirds of all mRNAs being represented (16, 21, 35). Between a quarter and a third of these maternal mRNAs are eliminated during the maternal-to-zygotic transition that occurs prior to cellularization 3 hours after fertilization (16, 21, 35, 37). Two degradation pathways direct elimination of these transcripts (3, 4). The first is termed the "maternal degradation pathway" because it is comprised of an exclusively maternally encoded machinery that is triggered upon egg activation, prior to fertilization (4, 36). The second, termed the "zygotic degradation pathway" since it requires both fertilization and zygotic transcription, initiates approximately 2 hours into embryonic development (4). The identification of these two decay activities allows maternal mRNAs to be categorized according to whether they are targeted exclusively by the maternal degradation pathway (e.g., *nanos* and *polar granule component*), exclusively by the zygotic degradation pathway (e.g., *hunchback*), by both activities (e.g., *Hsp83* and *string*), or by neither (e.g., *rpA1*, *rp49*, and α*Tub84B*) (4, 16, 30, 31, 35, 36).

A major regulator of transcript destabilization is the RNA-binding protein SMAUG (SMG), whose function is required for elimination of two-thirds of the mRNAs attacked by the maternal pathway (35). Analyses of *Hsp83* mRNA have shown that SMG acts as a specificity factor, recruiting the CCR4-NOT deadenylase, thus initiating decay through deadenylation (30). SMG's *s*terile-*a*lpha *m*otif (SAM) domain binds to specific stem-loops termed *S*MG *r*ecognition *e*lements (SREs) (2, 11–13, 32, 33). However, mutation of four computationally predicted SREs in the open reading frame (ORF) of *Hsp83* had no effect on the kinetics of transcript decay (30), raising several possibilities: that additional SREs might reside in the *Hsp83* mRNA, that SMG recognizes a novel *cis* element in the *Hsp83* mRNA, or that SMG's interaction with *Hsp83* mRNA is indirect. Subsequent to those analyses it was shown that VTS1, the *Saccharomyces cerevisiae* homolog of SMG, can bind to SREs with a loop up to 7 nucleotides (nt) long, $CNGGN_{0-3}$ (1). In addition, the crystal structure indicated that SRE binding

* Corresponding author. Mailing address: Department of Molecular Genetics, University of Toronto, Medical Sciences Building, Room 4384D, 1 King's College Circle, Toronto, Ontario M5S 1A8, Canada. Phone: (416) 946-5296. Fax: (416) 971-2494. E-mail: howard.lipshitz@utoronto.ca.

† Supplemental material for this article may be found at http://mcb.asm.org/.

▽ Published ahead of print on 15 September 2008.

involves limited sequence specificity, through recognition of the G residue at position 3 of the loop, in combination with recognition of the tertiary structure of the SRE (1). Thus, sequences that adopt a similar shape and contain a G residue in the correct context—but do not match the current SRE consensus—could, in principle, also be bound by VTS1/SMG (1).

Given the complexity of VTS1/SMG transcript recognition, here we took an unbiased approach to mapping the *cis* elements in the *Hsp83* mRNA that are required for destabilization, using hybrid transgenic mRNAs that fused parts of the *Hsp83* mRNA to parts of a stable mRNA, *rpA1*. These hybrid mRNAs enabled us to test different parts of the *Hsp83* transcript for a role in mRNA destabilization via the maternal degradation machinery (i.e., in unfertilized eggs) and via SMG (i.e., in *smg* mutants). Using this strategy, we mapped a major instability element—which we have termed the *Hsp83* mRNA *i*nstability *e*lement (HIE)—within the ORF. The HIE is sufficient to strongly destabilize *rpA1* mRNA when inserted into its ORF. The presence of the HIE within the ORF suggested that translation of the *Hsp83* mRNA might be required for transcript destabilization. However, the HIE retained its activity as an instability element even when inserted into a 3′ untranslated region (UTR), indicating that translation is not needed. We show that the HIE functions together with auxiliary elements in the more 5′ part of the *Hsp83* ORF as well as in its 3′ UTR to direct transcript destabilization. One of these auxiliary elements is the previously identified *Hsp83 d*egradation *e*lement (HDE), a 97-nt region within the *Hsp83* 3′ UTR (4).

Eight computationally predicted SREs are present in the *Hsp83* mRNA; all reside in its ORF, and six map to the HIE. We show that the HIE is sufficient to direct association with SMG protein as well as to confer SMG-dependent transcript instability. A single-amino-acid substitution that abrogates SMG's ability to bind SREs prevents *Hsp83* transcript destabilization. Furthermore, simultaneous mutation of all eight predicted SREs (without substantially altering the coding capacity of the ORF) stabilizes the transcript. We conclude that SMG binds directly to the *Hsp83* mRNA's ORF, thus recruiting the CCR4-NOT deadenylase and triggering transcript elimination despite the fact that *Hsp83* transcripts are actively translated.

MATERIALS AND METHODS

Fly stocks. *Drosophila melanogaster* wild-type stocks included *y* w^{1118} and w^{1118}. Both of these genetic backgrounds were used for the generation of transgenic lines. Expression of pUASP constructs was induced using *P[GAL4::VP16-nos.UTR]* (41). Due to the presence of a recessive lethal mutation(s) on the smg^1 chromosome, *smg* mutants were $smg^1/Df(3L)Scf^{R6}$ (12). In some cases, a transgenic P element insertion and the smg^1 allele were recombined onto the same chromosome, which resulted in the loss of the recessive lethal mutation, and thus, *smg* mutants were smg^1/smg^1. These genetic backgrounds are noted in the text.

Construction of transgenes. (i) H-H-H. The construct H-H-H was designed by Arash Bashirullah and contains the full-length *Hsp83* transcript with a p53 epitope tag inserted 3′ to the start codon. This transgene was constructed by Vent polymerase PCR of three fragments. The first *Hsp83* fragment, H**, contained the 5′ genomic region (876 nt), the 5′ UTR (149 nt), the intron (1,129 nt), and start codon, flanked with a 5′ BamHI site and a 3′ ApaI site. The second *Hsp83* fragment, *H*, was designed to contain the entire ORF with no start codon but with the stop codon (2,151 nt) and the first 6 nt of the 3′ UTR. This fragment was flanked with a 5′ ApaI site while two nucleotides, GC, were introduced between the +2 and +3 positions of the 3′ UTR to generate a 3′ AatII site. The third *Hsp83* fragment, **H, was designed to contain the 3′ UTR (407 nt) and downstream genomic DNA (1,281 nt total) flanked by 5′ AatII and 3′ KpnI sites. These three PCR fragments were subcloned into pBAAK, which is a modified pBluescript-SK vector that contained ApaI and AatII sites between the BamHI and KpnI sites, by digestion with HindIII/KpnI and insertion of annealed oligonucleotides *Apa-Aat-F* and *Aat-Apa-R* (all oligonucleotide sequences are listed in Table S1 in the supplemented material). The 5′ fragment was first cloned into pBAAK at the BamHI/ApaI sites, generating pBAAK-H**, and the 3′ fragment was subsequently cloned at AatII/KpnI sites to generate pBAAK-H*H. The final fragment, the ORF, was then cloned into pBAAK-H*H at ApaI/AatII sites to generate pBAAK-H-H-H. An N-terminal p53 tag was introduced at the ApaI site using annealed oligonucleotides *p53-F* and *p53-R*, thus generating an 8-amino-acid insertion immediately downstream of the start codon (the p53 epitope contains five residues). The insertion of this oligonucleotide duplex destroyed the first ApaI site and maintained the second site.

(ii) R-R-R. The construct R-R-R was designed with a strategy similar to that for H-H-H and used a full-length 2.7-kb genomic BamHI-BamHI *rpA1* fragment (gift of Marcello Jacobs-Lorena) which was subcloned into pBluescript-SK (collapsed at SalI/XhoI sites) and subsequently used as a PCR template for the following fragments. The first *rpA1* fragment, R**, was generated to contain the 5′ BamHI site, 5′ flanking genomic DNA (~1 kb), the 5′ UTR (89 nt), the start codon, the p53 tag, and an ApaI site. This fragment was PCR generated by Accuprime Pfx polymerase (Invitrogen) using primers *R5-Bam-5gen-F* and *R5-Apa-p53-R* and subsequently cloned into pBAAK at BamHI/ApaI sites to generate pBAAK-R**. The second *rpA1* fragment, *R*, contained the entire ORF, minus the start codon but including the stop codon (339 nt), and was flanked by a 5′ ApaI site and a 3′ AatII site. This second fragment was PCR generated via Elongase (Invitrogen) utilizing the primers *RO-Apa-F* and *RO-Aat-R* and was cloned into pBAAK at ApaI/AatII sites to generate pBAAK-*R*. The third *rpA1* fragment,**R, contained the entire 3′ UTR (168 nt) and 3′ flanking genomic DNA (~1 kb) flanked by 5′ AatII and 3′ KpnI sites and was PCR generated using Accuprime Pfx polymerase (Invitrogen) and primers *R3-Aat-F* and *R3-Bam-R*. This third fragment contained a BamHI site at the 3′ end just upstream of the flanking KpnI site. The third fragment was cloned into pBAAK at ApaI/KpnI sites to generate pBAAK-**R. Once all three fragments were individually cloned into pBAAK, the vector pBAAK-R-R-R was constructed via sequential digestion and ligation of ApaI-AatII-digested pBAAK-*R* and AatII-KpnI digested pBAAK-**R fragments into the ApaI-KpnI-digested pBAAK-R** backbone.

(iii) H/R hybrid constructs. The following constructs were generated from the appropriate digestions and ligations of the BamHI-ApaI 5′ fragment, the BamHI-AatII 5′+ ORF fragment, the ApaI-AatII ORF fragment, the ApaI-KpnI ORF +3′ fragment, or the AatII-KpnI 3′ fragment from the vectors pBAAK-H-H-H and pBAAK-R-R-R: pBAAK-H-H-R, pBAAK-H-R-R, pBAAK-H-R-H, pBAAK-R-R-H, pBAAK-R-H-R, and pBAAK-R-H-H.

(iv) H-H-H$^{\Delta HDE}$ and H-H$^{\Delta HORF4}$-H$^{\Delta HDE}$. The AatII-KpnI fragment of pBAAK-H-H-H and that of pBAAK-H-H$^{\Delta HORF4}$-H (see below), respectively, each containing the full-length *Hsp83* 3′ UTR, were replaced by a corresponding AatII-KpnI fragment from pBluescript-ΔHDE vector. This fragment contained the 97-nt deletion of the HDE, and its construction has been described previously (4). For R-R^{lacZ}-R, a 621-nt fragment of the *lacZ* coding sequence was PCR generated with flanking SalI sites and inserted in frame into the unique SalI site of the *rpA1* ORF within the full-length 2.7-kb genomic BamHI-BamHI *rpA1* fragment in pBluescript-SK (collapsed at SalI/XhoI sites) as described above. For R-R^{lacZ}-R^{HDE}, the BamHI-BamHI fragment of R-R^{lacZ}-R was subcloned into pUC18. In this vector backbone, a polylinker was inserted into the *rpA1* 3′ UTR at the NgoMI site, which introduced AvrII and BglII sites using the annealed oligonucleotides *AvrII-BglII-F* and *BglII-AvrII-R*. The HDE was PCR generated with flanking 5′ AvrII and 3′ BglII sites and subcloned into the same sites in pUC18-R-R^{lacZ}-R to generate pUC18-*rpA1-lacZ*+HDE.

(v) R-R^{HORF}-R. Four overlapping fragments of the *Hsp83* ORF (named HORF1 through HORF4 shifting 5′ to 3′) were PCR generated using Elongase (Invitrogen) and were flanked with XhoI sites. The vector pCSR4-H-H-H was used as the template (see below for construction of pCSR4 vectors). Each fragment contained 612 nt of *Hsp83* ORF sequence with the exception of HORF4, which contained 615 nt of the 3′-most region of coding sequence. The primers *Xho-HORF1-F* and *Xho-HORF1-R* were used for generating HORF1, the primers *Xho-HORF2-F* and *Xho-HORF2-R* were used for generating HORF2, the primers *Xho-HORF3-F* and *Xho-HORF3-R* were used for generating HORF3, and the primers *Xho-HORF4-F* and *Xho-HORF4-R* were used for generating HORF4. Each XhoI-digested PCR fragment was cloned into the unique SalI site contained within the *rpA1* ORF of pBAAK-R-R-R to generate the following constructs: pBAAK-R-R^{HORF1}-R, pBAAK-R-R^{HORF2}-R, pBAAK-R-

R^{HORF3}-R, and pBAAK-R-R^{HORF4}-R. The use of flanking XhoI sites in the primer sequences introduced amino acids VE at the 5′ junction between *rpA1* and *Hsp83* coding sequences (i.e., at the 5′ collapsed SalI site) and amino acids LD at the 3′ junction between *Hsp83* and *rpA1* coding sequences (i.e., at the preserved SalI site). These insertions maintained both the *rpA1* and *Hsp83* reading frames.

(vi) R-$R^{HORF4\text{-}X}$-R. Six overlapping subfragments (~120 nt each) of the HORF4 coding region were PCR generated using *Taq* polymerase (Amersham) and flanked with XhoI sites (fragment 4-7 was synthesized using Elongase [Invitrogen]). The vector pCSR4-H-H-H was used as the template (see "P-element transformation" below for construction of pCSR4 vectors). These six fragments overlap by ~20 nt with one another and were named HORF4-1 through HORF4-6 shifting 5′ to 3′ along the HORF4 region. The primers *Xho-HORF4-F* and *Xho-HORF4-1-R* were used for generating HORF4-1. The primers *Xho-HORF4-n-F* and *Xho-HORF4-n-R* were used to generate HORF4-*n*, where $2 \leq n \leq 5$. The primers *Xho-HORF4-6-F* and *Xho-HORF4-R* were used for generating HORF4-6. The HORF4 coding region was also subdivided into two larger overlapping fragments that were ~320 nt each and contained a ~20-nt overlap. These subfragments were named HORF4-7 and HORF4-8 (with the former representing the 5′-most fragment of the HORF4 region), were also PCR generated via *Taq* polymerase (Amersham), and were flanked with XhoI sites. The primers *Xho-HORF4-F* and *Xho-HORF4-3-R* were used for generating HORF4-7, and the primers *Xho-HORF4-4-F* and *Xho-HORF4-R* were used for generating HORF4-8. Each XhoI-digested PCR fragment was cloned into the unique SalI site contained within the *rpA1* ORF of pBAAK-R-R-R to generate the following constructs: pBAAK-R-$R^{HORF4\text{-}1}$-R, pBAAK-R-$R^{HORF4\text{-}2}$-R, pBAAK-R-$R^{HORF4\text{-}3}$-R, pBAAK-R-$R^{HORF4\text{-}4}$-R, pBAAK-R-$R^{HORF4\text{-}5}$-R, pBAAK-R-$R^{HORF4\text{-}6}$-R, pBAAK-R-R-$R^{HORF4\text{-}7}$-R, and pBAAK-R-$R^{HORF4\text{-}8}$-R. The use of flanking XhoI sites in the primer sequences introduced amino acids VE at the 5′ junction between *rpA1* and *Hsp83* coding sequences (i.e., at the 5′ collapsed SalI site) and amino acids LD at the 3′ junction between *Hsp83* and *rpA1* coding sequences (i.e., at the preserved SalI site). These insertions maintained both the *rpA1* and *Hsp83* reading frames.

(vii) R-R-R^{HORF4}. The HORF4 fragment was inserted in both sense and antisense orientations at two different unique restriction sites within the *rpA1* 3′ UTR in the vector pBAAK-R-R-R. The HORF4 fragment was generated by Elongase PCR (Invitrogen) and was flanked either with AatII sites using primers *Aat-HORF4-F* and *Aat-HORF4-R* or with FseI sites using primers *Fse-HORF4-F* and *Fse-HORF4-R*. The vector pCSR4-H-H-H was used as the PCR template (see below for construction of pCSR4 vectors). These two fragments were digested with their appropriate restriction enzymes, i.e., either digested with AatII and subsequently ligated into the AatII site in pBAAK-R-R-R (which is immediately following the stop codon) or digested with FseI and subsequently ligated into the FseI site just upstream of the poly(A) signal in the *rpA1* 3′ UTR in pBAAK-R-R-R. This resulted in the construction of pBAAK-R-R-$R^{sHORF4(Aat)}$, pBAAK-R-R-$R^{asHORF4(Aat)}$, pBAAK-R-R-$R^{sHORF4(Fse)}$, and pBAAK-R-R-$R^{asHORF4(Fse)}$.

(viii) H-$H^{\Delta HORF4}$-H. The construct pBAAK-H-H-H was digested at unique Bsu36I and AatII sites, which deleted a 528-nt fragment of the *Hsp83* coding region containing the majority of HORF4 (615 nt). The oligonucleotides *H4-Bsu-Aat-F* and *H4-Aat-Bsu-R* were annealed and ligated into the digested pBAAK-H-H-H vector to generate pBAAK-H-$H^{\Delta HORF4}$-H. A stop codon in the oligonucleotide duplex truncated the *Hsp83* ORF after codon 541 of the 717-amino-acid HSP83 protein. For R-$H^{\Delta HORF4}$-R, the ApaI-AatII fragment of pBAAK-H-$H^{\Delta HORF4}$-H was ligated into ApaI/AatII-digested pBAAK-R-R-R to generate pBAAK-R-$H^{\Delta HORF4}$-R. For H-$H^{\Delta HORF4+lacZ}$-H, a 528-nt *lacZ* ORF fragment that contained flanking 5′ Bsu36I and 3′ AatII sites was PCR generated using *Taq* polymerase (Amersham) and primers *LacZ-Bsu-F* and *LacZ-Aat-R*. This PCR *lacZ* fragment and the vector pBAAK-H-H-H were both digested with Bsu36I and AatII and ligated together to generate pBAAK-H-$H^{\Delta HORF4+lacZ}$-H. The *lacZ* PCR fragment was partially digested with Bsu36I, as it also contains a Bsu36I site internal to the primer sequences, and thus, the full-length *lacZ* fragment was maintained. The construct *Hsp83-lacZ* (H-$H^{\Delta 1.8kb+lacZ}$-H) has been previously described (4, 10). Briefly, the *Hsp83* 5′ genomic region, 5′ UTR, intron, and first 333 nt were fused to a 603-nt truncated fragment of the *lacZ* ORF. The 3′ end of the *lacZ* ORF was flanked with AatII and KpnI sites in which the same AatII-KpnI fragment described for the generation of H-H-H was used to insert the full-length *Hsp83* 3′ UTR and downstream genomic region. Thus, this construct created a ~1.8-kb deletion of the *Hsp83* ORF which was replaced with a *lacZ* fragment. The *lacZ* fragment did not, however, contain a stop codon and thus allowed translation to proceed into the *Hsp83* 3′ UTR.

Translation constructs. Oligonucleotide pairs were annealed and inserted at the unique BsiWI site within the *Hsp83* 5′ UTR of pCSR4-H-H-H. All oligonucleotide duplexes maintained the 5′ BsiWI site but eliminated the 3′ BsiWI site when inserted into BsiWI-digested pCSR4-H-H-H. For the generation of the $H^{hairpin}$-H-H construct, the 75-nt oligonucleotides *Hsp83-5′HP-F* and *Hsp83-5′HP-R* were designed to include the strong *hp7* hairpin sequence (20, 29) and annealed according to the Promega protocol for cloning a hairpin insert into pGeneClip vectors (Promega). These oligonucleotides contained NotI sites immediately internal to the BsiWI sites and also introduced a unique SacII site into the vector. H^{random}-H-H was produced by inserting the BsiWI-digested product of an Elongase PCR-amplified fragment of pCSR4 using the oligonucleotides *Bsi-CSR-F* and *Bsi-CSR-R* into the BsiWI site of pCSR-H-H-H. The 75-nt random sequence from the pCSR4 vector introduced an additional HindIII site which aided detection of positive transformants.

pUASP-SMG rescue constructs. The generation of the SMG^{RBD} point mutation A642H has been previously described (2). Both wild-type and point-mutated (A642H) *smg* cDNA fragments containing the ORF and 3′ UTR were cloned into the pUASP vector (27).

H-$H^{8xSRE(-)}$-H. Four overlapping fragments of the *Hsp83* ORF were PCR generated using Accuprime Pfx (Invitrogen). The vector 4xSRE$^-$ pCSR4-H-H-H (30) was used as the template. The primers *Apa-HORF1-F* and *H-SRE 3&4-R* were used to generate 1.1614, *H-SRE 3&4-F* and *H-SRE 6-R* were used for 1567.1953, *H-SRE 6-F* and *H-SRE 8-R* were used for 1929.2100, and *H-SRE 8-F* and *Hsp83 3U100-3H* were used for 2095.3U-100. Accuprime Pfx, primer *Apa-HORF1-F*, *Hsp83 3U100-3H*, and 1 μl of each gel-purified fragment were used to PCR generate 8xSRE(-) Hsp83 ORF+3U-100. Gel-purified PCR fragment was cloned into the pCR21.TOPO vector. ApaI- and AatII-digested 8xSRE(-) HORF fragment was subcloned into the same site in pBAAK-H-H-H to replace the wild-type HORF and generate the 8xSRE(-) pBAAK-H-H-H, the mRNA from which is referred to in the text as H-$H^{8xSRE(-)}$-H.

P-element transformation. All NotI-KpnI inserts from the pBAAK vectors described above (i.e., containing the 5′, p53 tag, ORF, and 3′ fragments) were then subcloned into pCSR4 (39) at NotI/KpnI sites. All inserts were sequenced in pBAAK and/or pCSR4 vectors (except for the full-length p53-tagged *Hsp83* construct, H-H-H, which was tested for its ability to rescue an *Hsp83* RNA null mutation and for wild-type mRNA decay kinetics [30]). The BamHI fragment from *rpA1-lacZ* in pBluescript-SK was subcloned into pCSR2 (39) at the BamHI site, while the BamHI fragment of *rpA1-lacZ*+HDE (R-R^{lacZ}-R^{HDE}) in pUC18 was subcloned into pCSR4 at its BamHI site. Germ line transformants were recovered using standard methods (28).

Northern, RNA dot blot, and real-time RT-PCR analysis. Fertilized embryo and unfertilized egg collections were performed at 25°C as previously described (4). Unfertilized eggs were derived from adult virgin females mated to *T(Y,2)* sterile males. RNase H cleavage assays, Northern blotting, and RNA dot blotting techniques were performed as previously described (4, 30). Briefly, total RNA was extracted from eggs/embryos collected at various time periods after egg lay (AEL) by homogenizing it in Trizol (Invitrogen) containing 250 μg/ml glycogen and following standard reagent protocols. For Northern blot analyses, samples containing either an equivalent number of eggs/embryos or an equivalent amount of total RNA were electrophoresed using 1% agarose-formaldehyde gels in 1× morpholinepropanesulfonic acid (MOPS) buffer and transferred overnight onto Hybond-N nylon membranes. For RNase H cleavage assays, samples containing 10 μg of total RNA were incubated with the oligonucleotide *Hsp83ORF.3* (for detection of H-H-$H^{\Delta HDE}$ mRNA) or the oligonucleotide *p53-Apa24.3* (for detection of R-R-R mRNA) in the presence of RNase H according to standard methods (15). Cleaved RNA samples containing H-H-$H^{\Delta HDE}$ mRNA were run on a 4% denaturing urea-polyacrylamide gel and electrotransferred overnight using the Trans-blot cell (Bio-Rad Laboratories) at 30 V while R-R-R mRNA samples were resolved using a 1.2% agarose-formaldehyde gel and transferred as described above. For RNA dot blots, total RNA was extracted from single embryos and blotted directly onto Hybond-N membrane in SSC (1× SSC is 0.15 M NaCl plus 0.015 M sodium citrate) buffer using the Schleicher & Schuell Minifold-I dot blot system according to the manufacturer's protocol (Schleicher & Schuell). All blots were UV cross-linked, hybridized overnight with random-primed radiolabeled probes, and exposed to a storage phosphor screen, which was then scanned using the STORM860 (Molecular Dynamics) phosphorimager. Quantification was performed using Imagequant software (Molecular Dynamics) and Excel (Microsoft Office). Real-time reverse transcription-PCR (RT-PCR) was performed as described previously (30).

To detect H-$H^{8xSRE(-)}$-H transcripts, a 19-base locked nucleic acid (LNA) probe specific to the sequence encoding the p53 tag was synthesized (5′-CCA CCA CGG AGT GGC GGC C-3′, where underlines indicate locked bases; the 3′ end was modified with digoxigenin). Gel running and transfer steps for RNA

were performed as described above. Hybridization followed the Exiqon microRNA LNA probe Northern protocol. Briefly, the membrane was prehybridized in RNA hybridization buffer (50% formamide, 0.5% sodium dodecyl sulfate [SDS], 5× SSPE [1× SSPE is 0.18 M NaCl, 10 mM NaH_2PO_4, and 1 mM EDTA (pH 7.7)], 5× Denhardt's solution, and 20 μg/ml sheared, denatured, salmon sperm DNA) for 30 to 60 min. Forty-eight picomoles of p53-LNA probe was heated for 1 minute at 95°C before being added to 7 ml hybridization buffer. The membrane was hybridized overnight with the LNA probe at 45°C in the same solution. After hybridization, membranes were washed with 2× SSC-0.1% SDS at 45°C twice for 5 minutes, then with 0.1× SSC-0.1% SDS at 59°C twice for 10 minutes. The digoxigenin luminescent detection kit (Roche 1363514) was used following Roche's protocol. Briefly, the membranes were blocked and incubated with antidigoxigenin-alkaline phosphatase antibody and then developed with CSPD. Membranes were exposed to an imaging device or to X-ray film. Quantification was performed using Imagequant software and Excel (Microsoft Office).

Real-time RT-PCR was performed as described previously (30). Embryos were disrupted in a minimal volume of buffer A (150 mM KCl, 20 mM HEPES, pH 7.4, 1 mM $MgCl_2$, 1 mM dithiothreitol [DTT], 1 mM aminoethylbenzenesulfonyl fluoride, 2 μg/ml leupeptin, 2 μg/ml pepstatin, 2 mM benzamidine). After centrifugation the supernatant was supplemented with glycerol to a final concentration of 10%, and 9 M urea (supplemented with 1 mM DTT, 1 mM aminoethylbenzenesulfonyl fluoride, 2 μg/ml leupeptin, 2 μg/ml pepstatin, 2 μM benzamidine) was added to 75 μl of extract to a 2 M final concentration. The extract was recentrifuged and added to 5 μl of protein G beads carrying either rat anti-SMG antibody or normal rat serum. Beads were incubated for 2 h at 4°C and washed several times in buffer A supplemented with urea. RNA was then purified from the beads using Trizol reagent (Invitrogen) and reverse transcribed using random primers and Superscript II (Invitrogen). Samples were subjected to real-time PCR using Sybr green master mix and the ABI Prism 7900 sequence detection system (Applied Biosystems).

Western blot analysis. Western blot analyses were carried out as previously described (30). Briefly, eggs/embryos were dechorionated in 50% bleach, rinsed and homogenized in lysis buffer (150 mM NaCl, 50 mM Tris, pH 7.5, 1% NP-40, 1 mM DTT, 1× EDTA-free protease inhibitor cocktail [Roche]), incubated on ice for 5 min, and then centrifuged for 5 min at 12,000 × *g* at 4°C. The supernatant was combined with 2× SDS loading dye, loaded, and subjected to SDS-polyacrylamide gel electrophoresis (7.5% acrylamide). The Bio-Rad Trans-blot SD semidry transfer cell was used to transfer proteins to a polyvinylidene difluoride membrane (Invitrogen). Blots were blocked in 1% skim milk powder before incubations with primary and secondary antibodies. Primary antibodies used were mouse monoclonal anti-p53 at 1:1,000 (Santa Cruz Biotechnology; SC-99), guinea pig polyclonal anti-SMG at 1:10,000 (35), and guinea pig polyclonal anti-DDP1 at 1:10,000 (24, 35). Secondary horseradish peroxidase-conjugated antibodies were used at 1:5,000 (Jackson ImmunoResearch Laboratories, Inc.). Chemiluminescence was detected using Pierce enhanced chemiluminescence Western blotting reagent and standard X-ray film.

RESULTS

The *Hsp83* ORF functions as a transcript instability element. To map *cis*-acting instability elements in the *Hsp83* mRNA, chimeric transgenes were constructed, each containing combinations of the 5′ UTR, ORF, and 3′ UTR of *Hsp83* and *rpA1*, a highly stable mRNA. The constructs are listed in Table 1; these, and additional ones used in subsequent experiments, encoded a five-residue p53 epitope tag immediately after the amino-terminal methionine unless otherwise noted. The stability profiles of the hybrid mRNAs were examined using Northern blot assays of total RNA extracted from staged unfertilized eggs laid by transgenic females at 0 to 2, 2 to 4, and 4 to 6 h AEL, thus enabling us to assess the role of the *cis* elements in the maternally encoded transcript degradation pathway.

The control *rpA1* transgenic transcript, R-R-R (where the first letter denotes the source of the 5′ UTR, the second the source of the ORF, and the third the source of the 3′ UTR), was highly stable, although less so than endogenous *rpA1* mRNA (Table 1) (for endogenous *rpA1*, 95% ± 21% of the transcripts remained at 4 to 6 h AEL, while for R-R-R 74% ± 5% remained). The R-H-R and R-R-H constructs were used to assess whether the *Hsp83* ORF or *Hsp83* 3′ UTR, respectively, was sufficient to destabilize *rpA1* mRNA while R-H-H and H-H-R were used to ask whether the corresponding regions were necessary for *Hsp83* mRNA decay. For technical reasons, the sufficiency of the *Hsp83* 5′ UTR could not be assayed in these experiments (see footnotes to Table 1); however, our subsequent experiments showed definitively that the 5′ UTR is not required for destabilization. Since 26% ± 5% of R-R-R mRNA was degraded by 4 to 6 h AEL, throughout this study we have used the following terminology to describe the results: instability was defined as "strong" if >50% of the mRNA was eliminated by 4 to 6 h AEL, "weak" if 30 to 50% was eliminated, and "none" if <30% was eliminated.

TABLE 1. The *Hsp83* ORF acts as a strong instability element

Transcript	% Degraded by 4–6 h AEL	Destabilization[a]
Endogenous and control transgenic transcripts		
Hsp83	92 ± 6	Strong
$H^{\Delta intron}$-H-H	87 ± 16	Strong
R-R-R	26 ± 5	None
rpA1	5 ± 21	None
Necessity hybrid transcripts		
R-H-H	78 ± 7	Strong
H-H-R	88 ± 4	Strong
$H^{\Delta intron}$-H-R	97 ± 1	Strong
H-R-H	NA[b]	
Sufficiency hybrid transcripts		
R-H-R	72 ± 7	Strong
R-R-H	36 ± 15	Weak
H-R-R	NA	

[a] Destabilization categories: strong, >50% degraded by 4 to 6 h AEL; weak, 30 to 50% degraded by 4 to 6 h AEL; none, <30% degraded by 4 to 6 h AEL.

[b] NA, not assayed. H-R-R and H-R-H were not testable because artifactual destabilization was found to occur when an exogenous 5′ UTR (either from *Hsp83* or from a stable mRNA, α*Tub84B*) was fused to the *rpA1* ORF (data not shown). Constructs with the *rpA1* 5′ UTR are intronless. To confirm that the lack of an intron did not alter transcript stability, intronless constructs $H^{\Delta intron}$-H-H and $H^{\Delta intron}$-H-R were made and shown to be strongly unstable.

The extent of mRNA destabilization produced by the necessity constructs, R-H-H (78% ± 7% degraded by 4 to 6 h AEL) and H-H-R (88% ± 4% degraded), was strong and comparable to that observed for endogenous *Hsp83* mRNA (92% ± 6%) (Table 1). With respect to sufficiency, the *Hsp83* ORF inserted into R-H-R was sufficient to strongly destabilize the hybrid transcripts, eliminating 72% ± 7% of the transcripts by 4 to 6 h AEL. In contrast, the effects of the *Hsp83* 3′ UTR on R-R-H were weak, eliminating 36% ± 15% of transcripts by the same stage. The region common to all of the hybrid transcripts that exhibited strong destabilization is the *Hsp83* ORF, consistent with the hypothesis that the ORF contains one or more transcript instability elements. The data are also consistent with the possibility that the 3′ UTR contains a weak instability element.

We note that an alternative to the "instability element" interpretation presented here is that the *rpA1* mRNA houses stabilization elements. For example, the R-H-R transcript

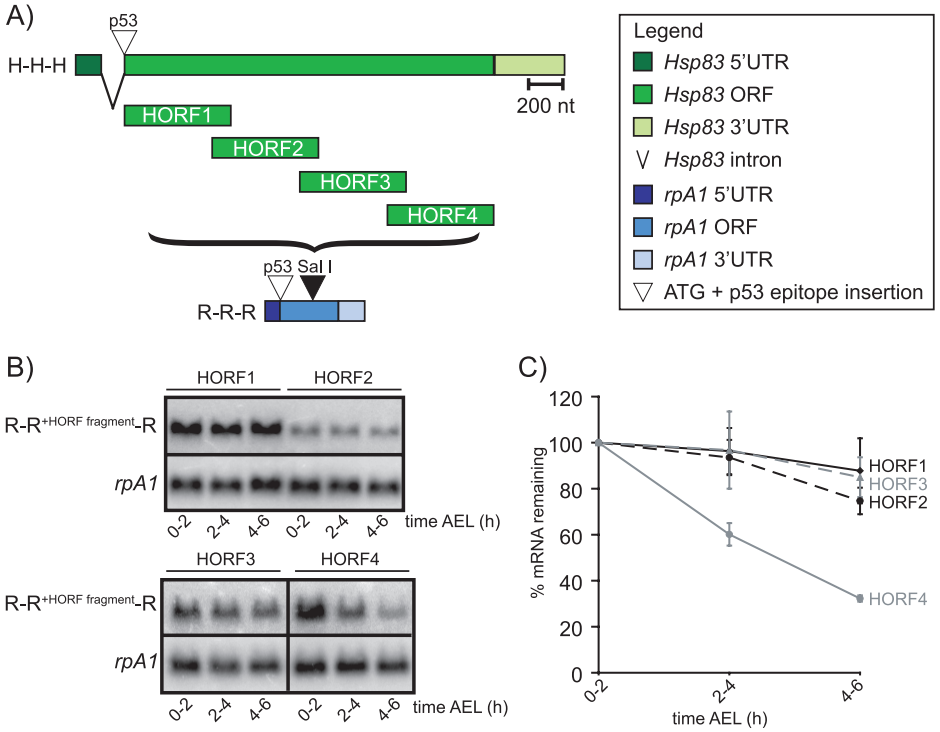

FIG. 1. A strong instability element—the HIE—maps within the *Hsp83* ORF. (A) Schematic representation of the *Hsp83* ORF sufficiency constructs. Four overlapping fragments (~615 nt each with 100-nt overlap) of the *Hsp83* coding sequence (HORF1 to HORF4) were independently inserted in frame into the transgenic R-R-R construct at a unique SalI restriction site within the *rpA1* coding sequence. Constructs are drawn to scale. (B) Northern blot analysis of the *Hsp83* ORF sufficiency constructs in unfertilized eggs. Blots were probed with the *rpA1* 3′ UTR to detect mRNA from both the transgene and the loading control, *rpA1*. (C) Quantification of Northern blot data in panel B. Average normalized transgenic mRNA levels between two or more independently derived transgenic fly lines are shown. Transgenic mRNA levels were normalized to loading controls. Error bars represent standard deviations calculated from at least two independent experiments. All experiments were performed using unfertilized eggs from transgenic mothers, collected at 0 to 2 h, 2 to 4 h, and 4 to 6 h AEL. Transcript levels at 2 to 4 h and 4 to 6 h AEL are represented as a percentage of the initial amount detected at 0 to 2 h (i.e., % mRNA remaining).

could be unstable due to loss of such elements. *rpA1* has been used previously as a backbone with which to map instability elements within the *bicoid* and *fushi tarazu* mRNAs (17, 19, 26, 34). Since the *bicoid* and *fushi tarazu* instability elements function in the presence of the *rpA1* 5′ UTR and/or ORF, we favor—and subsequent experiments presented below support—the interpretation that the *Hsp83* mRNA contains instability elements.

A 615-nt HIE resides within the ORF. To refine the mapping of the strong instability element(s) within the *Hsp83* ORF, four overlapping fragments that together spanned the entire 2,154 nt were inserted in frame into the ORF of R-R-R (Fig. 1A). These fragments were each ~615 nt long and overlapped by ~100 nt. The stability of the resulting hybrid mRNAs was assayed in unfertilized eggs as described above. The fourth fragment, HORF4, was sufficient to strongly destabilize R-R-R mRNA, eliminating 68% ± 1% of transcripts by 4 to 6 h AEL, while the other fragments—HORF1 (12% ± 14%), HORF2 (25% ± 6%), and HORF3 (15% ± 9%)—had no significant destabilizing activity (Fig. 1B and C). That all four fragments of the *Hsp83* ORF were inserted at the same site within the R-R-R ORF and yet only HORF4 destabilized the hybrid mRNA supports the hypothesis that the instability of R-R^{HORF4}-R transgenic mRNA is due to the presence of the HORF4 sequence and not to an effect of the insertion site. Consistent with this conclusion, insertion of a piece of the *lacZ* ORF into this same site did not significantly destabilize the mRNA (see R-R^{lacZ}-R below and Fig. 4I and J).

These results demonstrate that the *Hsp83* ORF houses a strong instability element within its 3′-most region (viz., nucleotide positions 1537 to 2154 in reference to the published *Drosophila Hsp83* cDNA sequence [6]). Since there was a ~100-nt overlap between HORF3 and HORF4, and HORF4 but not HORF3 could trigger strong destabilization, the major instability element is likely to reside within the last 516 nt of the *Hsp83* ORF. However, since we cannot rule out the possibility that the 3′ limit of HORF3 fragment disrupts an instability element that spans this boundary, we have called the entire 615-nt HORF4 fragment the HIE. The identification of the HIE is consistent with a conclusion reached above: that a major instability element resides within the *Hsp83* mRNA coding region. Furthermore, if there are stabilization elements present within the *rpA1* transcript, the HIE is able to override their stabilizing functions.

To dissect the HIE further, six subfragments spanning the entire HIE were generated and named HORF4-1 through HORF4-6 (Fig. 2A). These subfragments were each ~120 nt long with an ~20-nt overlap and were inserted into R-R-R as described above. In addition, two larger subfragments of the HIE, which were each ~320 nt long with ~20 nt of overlap,

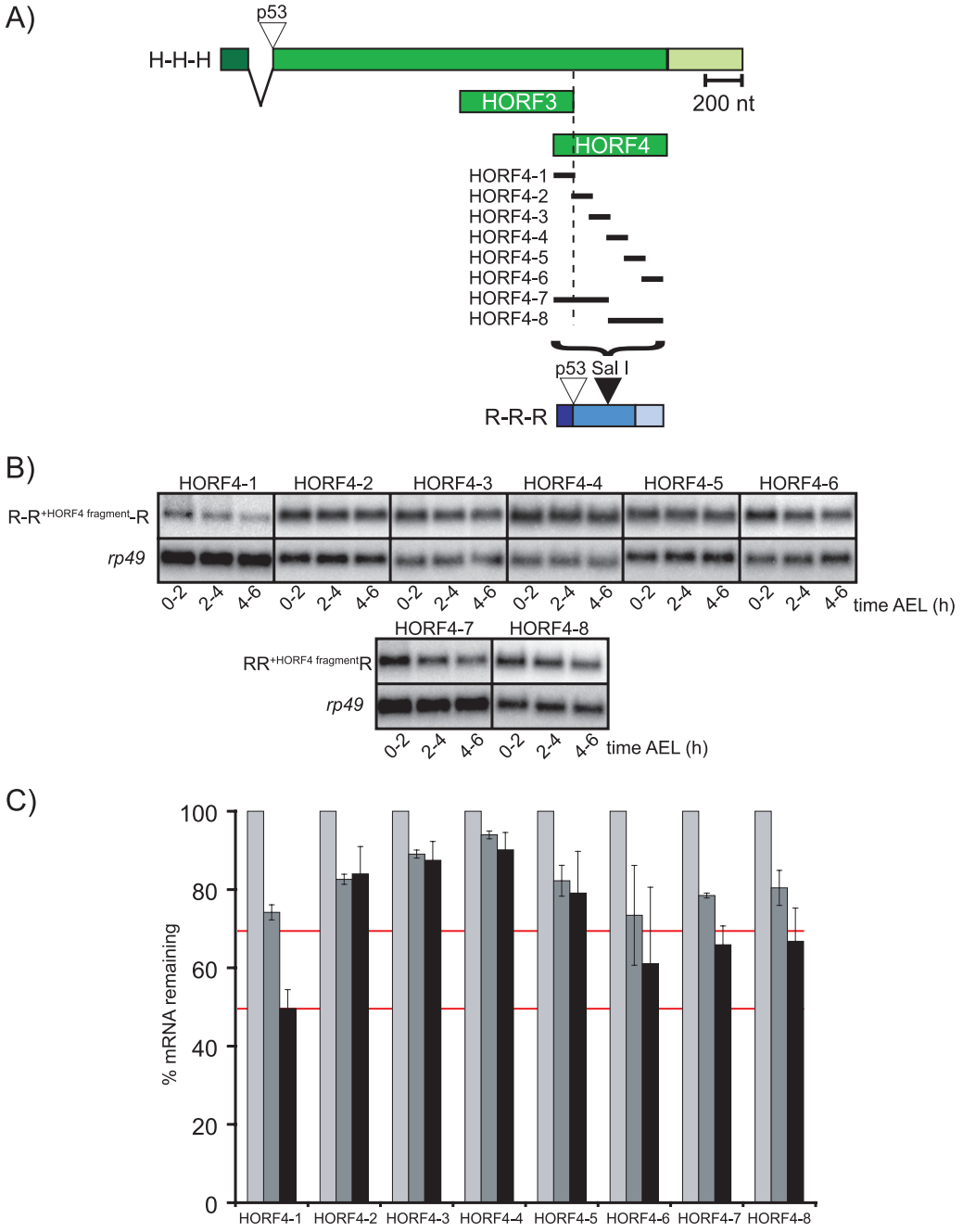

FIG. 2. Several subfragments of the HIE confer moderate instability. (A) Schematic representation of the HORF4 subfragments utilized to study the HIE. Six overlapping fragments (~100 nt each with 20-nt overlap) as well as two larger overlapping fragments (~320 nt each with 20-nt overlap) of the HORF4 region (HORF4-1 to HORF4-8) were independently inserted into the transgenic R-R-R construct at a unique SalI restriction site within the *rpA1* coding sequence. All HORF fragments were inserted in frame into R-R-R. Constructs are drawn to scale. (B) Northern blot analysis of the HORF4 subfragment sufficiency constructs in unfertilized eggs. Blots were probed with the HORF4 fragment of the *Hsp83* ORF to detect transgenic mRNAs and with the loading control, *rp49*. (C) Quantification of Northern blot data in panel B. Average normalized transgenic mRNA levels between two independently derived transgenic fly lines are shown. Egg collection time points were the same as those for Fig. 1, and normalization was performed as described for Fig. 1. Light grey, 0 to 2 h AEL; dark grey, 2 to 4 h AEL; black, 4 to 6 h AEL. The red lines indicate the cutoffs defined in the text for lack of destabilizing ability (above the upper red line), weak destabilizing ability (between the red lines), and strong destabilizing ability (below the lower red line) at the 4- to 6-h time point.

were inserted in frame into the R-R-R ORF (HORF4-7 and HORF4-8) (Fig. 2A). None of the subfragments of the HIE was capable of recapitulating the strong destabilization accomplished by insertion of the entire HIE (Fig. 2B and C). A weak destabilizing effect was observed by 4 to 6 h upon insertion of HORF4-1 (50% ± 5% mRNA eliminated), HORF4-6 (39% ± 20% eliminated), HORF4-7 (34% ± 5% eliminated), and HORF4-8 (33% ± 9% eliminated). Transcripts carrying

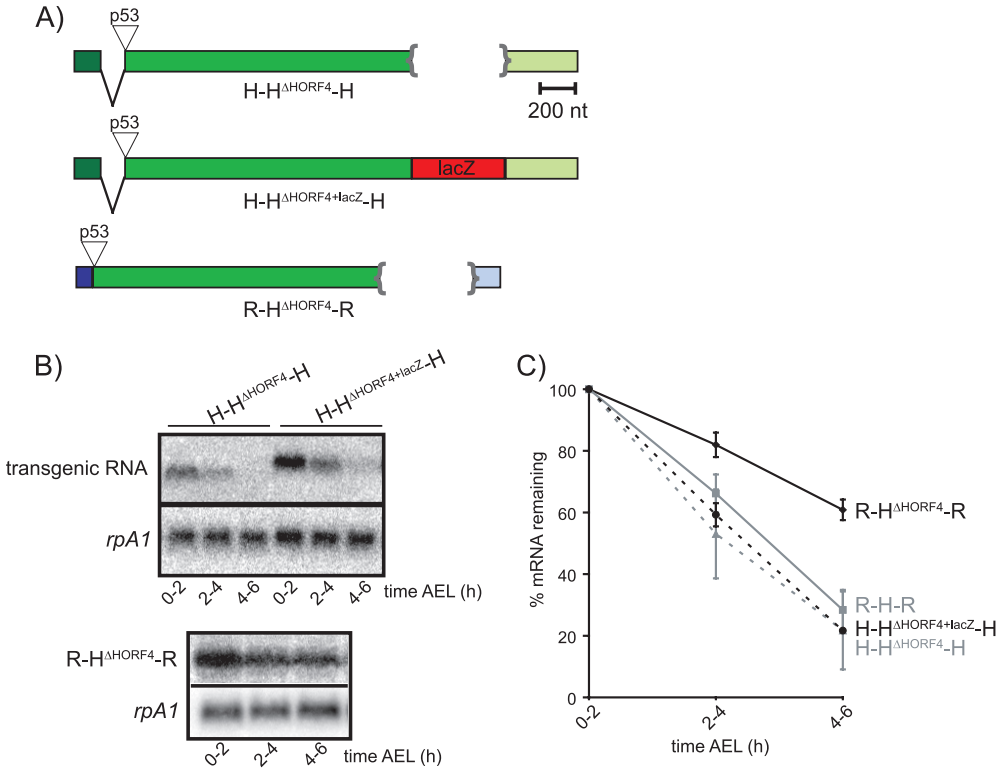

FIG. 3. The HIE is not necessary for destabilization of full-length *Hsp83* transgenic mRNA but is required for the destabilization of R-H-R transgenic mRNA. (A) Schematic representation of necessity constructs. These constructs all contained a deletion within the *Hsp83* coding sequence that removes the majority of the HIE (the 5′-most 87 nt of HIE are still present). This 3′-most 528-nt region of the *Hsp83* coding sequence was deleted within full-length H-H-H (top), was replaced with 528-nt *lacZ* coding sequence within full-length H-H-H (middle), and was deleted within the transgenic construct R-H-R (bottom). (B) Northern blot analysis of H-H$^{\Delta HORF4}$-H, H-H$^{\Delta HORF4+lacZ}$-H, and R-H$^{\Delta HORF4}$-R mRNAs in unfertilized eggs. H-H$^{\Delta HORF4}$-H and H-H$^{\Delta HORF4+lacZ}$-H mRNAs were detected by probing for the p53 sequence, and *rpA1* mRNA was used as a loading control. For R-H$^{\Delta HORF4}$-R, probing was with the *rpA1* 3′ UTR, which detected both the transgenic mRNA and the loading control, *rpA1*. (C) Quantification of Northern blot data in panel B. Average normalized transgenic mRNA levels between two independently derived transgenic fly lines are shown.

HORF4-2, HORF4-3, HORF4-4, and HORF4-5 were stable since only 16% ± 7%, 13% ± 5%, 10% ± 4%, and 21% ± 11% of the respective transcripts were eliminated by 4 to 6 h AEL.

The inability to uncover a single subfragment of the HIE that produced a strong decay profile resembling that of the entire HIE, along with the weak destabilizing effect of several subfragments, suggests that the HIE contains two or more subelements that function in combination, possibly additively, to mediate strong transcript degradation. The weak destabilizing activity of HORF4-1 and HORF4-6 supports the notion that most of these subelements reside toward the ends, rather than the central region, of the HIE. Consistent with this hypothesis, weak degradation was also induced by each of the larger subfragments, HORF4-7 and HORF4-8, which include HORF4-1 and HORF4-6, respectively.

The HIE is not necessary for the destabilization of full-length *Hsp83* mRNA. To assess the role of the HIE in the context of the *Hsp83* mRNA, we constructed a transgene, H-H$^{\Delta HORF4}$-H, in which the majority of the HIE was removed (i.e., the 3′-most 528 nt of the 615-nt HIE) (Fig. 3A). To ensure that any observed instability was not a consequence of shortening the length of the ORF, a "substitution" construct was also made, in which the deleted 528 nt were replaced with 528 nt of the *lacZ* coding sequence fused in frame to the *Hsp83* ORF (H-H$^{\Delta HORF4+lacZ}$-H) (Fig. 3A). Both the H-H$^{\Delta HORF4}$-H and H-H$^{\Delta HORF4+lacZ}$-H transgenic mRNAs were strongly unstable: 78% ± 13% of the H-H$^{\Delta HORF4}$-H transcripts were eliminated by 4 to 6 h AEL while 78% ± 0% of H-H$^{\Delta HORF4+lacZ}$-H transcripts were eliminated (Fig. 3B and C). Thus, the 528-nt fragment of the HIE is not necessary for H-H-H mRNA degradation, likely because of additional instability elements elsewhere in the *Hsp83* mRNA.

To assess the necessity of the HIE in the absence of additional *Hsp83* mRNA instability elements, we next examined the 528-nt deletion of the HIE within the context of the R-H-R transgene, which lacks the *Hsp83* 5′ UTR and 3′ UTR (Fig. 3A). Transgenic R-H$^{\Delta HORF4}$-R transcripts were substantially stabilized relative to R-H-R but did remain weakly unstable (39% ± 3% eliminated versus 72% ± 7%, respectively) (Fig. 3B and C).

Together, our results support the hypothesis that the HIE is a major instability element that can function to strongly destabilize an otherwise stable mRNA (R-R-R). The weak instability of R-H$^{\Delta HORF4}$-R mRNA is consistent with additional, minor instability elements residing in the undeleted part of the *Hsp83* ORF. Furthermore, the fact that the HIE is necessary to mediate strong degradation in the R-H-R context but not in the full-length H-H-H context is consistent with additional

instability elements mapping outside the ORF, possibly in the 3′ UTR, which exerts weak destabilizing activity (Table 1).

A large deletion in the *Hsp83* ORF substantially stabilizes the mRNA. Given the inference that weak instability elements might reside in the *Hsp83* ORF upstream of the HIE, we next assessed whether a large deletion within the ORF would stabilize the mRNA to a greater extent than deletion of the HIE alone. We previously reported that an *Hsp83-lacZ* hybrid mRNA containing the *Hsp83* 5′ UTR, the first 333 nt of the ORF (fused in frame to a fragment of the *lacZ* ORF), and the full-length *Hsp83* 3′ UTR is unstable in early embryos (4). To assess whether this 1,821-nt deletion, which removes more than 80% of the ORF, affects transcript stability via the maternal decay pathway, we examined the *Hsp83-lacZ* reporter mRNA—here renamed H-H$^{\Delta 1.8kb+lacZ}$-H to be consistent with the nomenclature used in the present study—in unfertilized eggs and found that it was partially stabilized (Fig. 4E and F): at 2 to 4 h AEL, 79% ± 10% of H-H$^{\Delta 1.8kb+lacZ}$-H mRNA remained compared to 14% ± 3% of endogenous *Hsp83* transcripts while, by 4 to 6 h, 31% ± 3% of H-H$^{\Delta 1.8kb+lacZ}$-H transcripts remained compared with only 2% ± 1% of endogenous transcripts. Thus, deletion of most of the *Hsp83* ORF, including the HIE, substantially (but incompletely) abrogates mRNA degradation via the maternal decay pathway.

The fact that H-H$^{\Delta 1.8kb+lacZ}$-H transcripts were partially stabilized relative to H-H$^{\Delta HORF4}$-H and H-H$^{\Delta HORF4+lacZ}$-H transcripts is consistent with the hypothesis that instability elements additional to the HIE reside in the more-5′ region of the *Hsp83* ORF. The fact that the H-H$^{\Delta 1.8kb+lacZ}$-H transcript was only weakly stabilized is consistent with additional instability elements mapping in the 3′ UTR.

An auxiliary instability element—the previously identified HDE—resides in the *Hsp83* 3′ UTR. We previously reported that deletion of a 97-nt region within the 407-nt 3′ UTR of *Hsp83*—the HDE—within the context of the H-H$^{\Delta 1.8kb+lacZ}$-H reporter mRNA (i.e., H-H$^{\Delta 1.8kb+lacZ}$-H$^{\Delta HDE}$) resulted in strong stabilization of this mRNA in unfertilized eggs (4). The HDE is, however, not necessary for degradation of *Hsp83* transcripts: deletion of the HDE in the context of a full-length *Hsp83* transgene (H-H-H$^{\Delta HDE}$) had no effect on transcript destabilization (Fig. 4A and B). That the HDE is not required for the decay of the *Hsp83* transcripts is consistent with our finding that H-H-R transcripts, in which the entire *Hsp83* 3′ UTR was replaced, remained highly unstable (Table 1).

We next assayed whether simultaneous deletion of the HIE and HDE (H-H$^{\Delta HORF4}$-H$^{\Delta HDE}$) had an effect on stability. Our results clearly indicated that there is no difference between the decay kinetics of H-H$^{\Delta HORF4}$-H and those of H-H$^{\Delta HORF4}$-H$^{\Delta HDE}$ transcripts: in the case of H-H$^{\Delta HORF4}$-H, 22% ± 13% of transcripts remained while, for H-H$^{\Delta HORF4}$-H$^{\Delta HDE}$, 21% ± 0% remained at 4 to 6 h AEL compared with <10% of endogenous mRNA (Fig. 4C and D).

As described in the previous section, transcripts carrying the large, 1.8-kb ORF deletion, H-H$^{\Delta 1.8kb+lacZ}$-H, are weakly stabilized, with 31% ± 3% remaining 4 to 6 h AEL (Fig. 4E and F). However, together with the HDE deletion (H-H$^{\Delta 1.8kb+lacZ}$-H$^{\Delta HDE}$), these were strongly stabilized with 66% ± 4% remaining at 4 to 6 h AEL (Fig. 4G and H).

Together, these data support the hypothesis that several instability elements for *Hsp83* mRNA—including a major element, the HIE—reside in its ORF and that the 3′-UTR-located HDE functions as an auxiliary instability element whose role is revealed only in the context of a sensitized transcript in which most, but not all, of the ORF-located elements are deleted.

The sufficiency experiments documented above are consistent with the hypothesis that the HDE is an auxiliary instability element, since weak destabilization was observed for R-R-H transgenic mRNA (Table 1). To specifically address the role of the HDE in mediating this destabilization, we inserted the HDE into the 3′ UTR of a transgene, R-R^{lacZ}-R, which comprises full-length genomic *rpA1* with a portion of the *lacZ* ORF inserted in frame into the *rpA1* coding sequence (to distinguish the transgenic transcripts from endogenous ones). R-R^{lacZ}-R was stable, with only 14% ± 20% eliminated by 4 to 6 h AEL (Fig. 4I and J). Insertion of the HDE (R-R^{lacZ}-R^{HDE}) had a weak destabilizing effect: 37% ± 14% of transgenic mRNA was eliminated by 4 to 6 h AEL (Fig. 4I and J), essentially identical to that seen for R-R-H (36% ± 15% eliminated) (Table 1).

We conclude that the HDE is an auxiliary instability element that functions together with the major instability elements, which are located in the *Hsp83* ORF.

Translation of the *Hsp83* mRNA and/or of the HIE is not required for transcript destabilization. We showed previously that *Hsp83* mRNA is actively translated in early embryos (30). To investigate whether translation of an *Hsp83* transcript is required to trigger its degradation, we inserted a strong, stable hairpin within the 5′ UTR of the full-length H-H-H transgene (position 18 of the 149-nt-long 5′ UTR) (Fig. 5A). The identical hairpin inserted anywhere between a 5′ cap and an initiation codon has been shown previously to block translation by preventing 40S ribosome subunit scanning in vitro and, thus, to efficiently block translation of c-*fos* mRNA in mouse NIH 3T3 cells (20, 29). To control for any potential stabilizing effect of disruption of the *Hsp83* 5′ UTR per se, an additional construct was made in which a random sequence of identical length was inserted at the same position (Fig. 5A). Both of these transgenic transcripts, H^{hairpin}-H-H and H^{random}-H-H, were examined for translational status and stability. Western blot analysis showed that, as expected, H^{random}-H-H mRNA was translated while H^{hairpin}-H-H was not (Fig. 5B). Thus, the insertion of the hairpin efficiently and specifically blocked translation. We next assessed the decay kinetics of H^{random}-H-H and H^{hairpin}-H-H mRNA (Fig. 5C and D). Both mRNAs were rapidly degraded over a 6-hour time course and exhibited decay kinetics similar to those of endogenous *Hsp83* mRNA. These results demonstrate that *Hsp83* mRNA translation in *cis* is not required for transcript degradation.

Our results using H^{hairpin}-H-H mRNA suggested that the HIE might not need to reside within the ORF for it to function as an instability element. Constructs were therefore made to assess the position dependence of the HIE by inserting it in both the sense and antisense orientations at two different sites within the 3′ UTR of R-R-R (Fig. 5E). In each of these, since the HIE was downstream of the translation stop codon, it was "protected" from ribosome transit. Insertion of the HIE at either site in its sense orientation conferred strong transcript instability: 77% ± 5% of R-R-R$^{sHORF4(Aat)}$ and 77% ± 9% of R-R-R$^{sHORF4(Fse)}$ transcripts were degraded by 4 to 6 h AEL

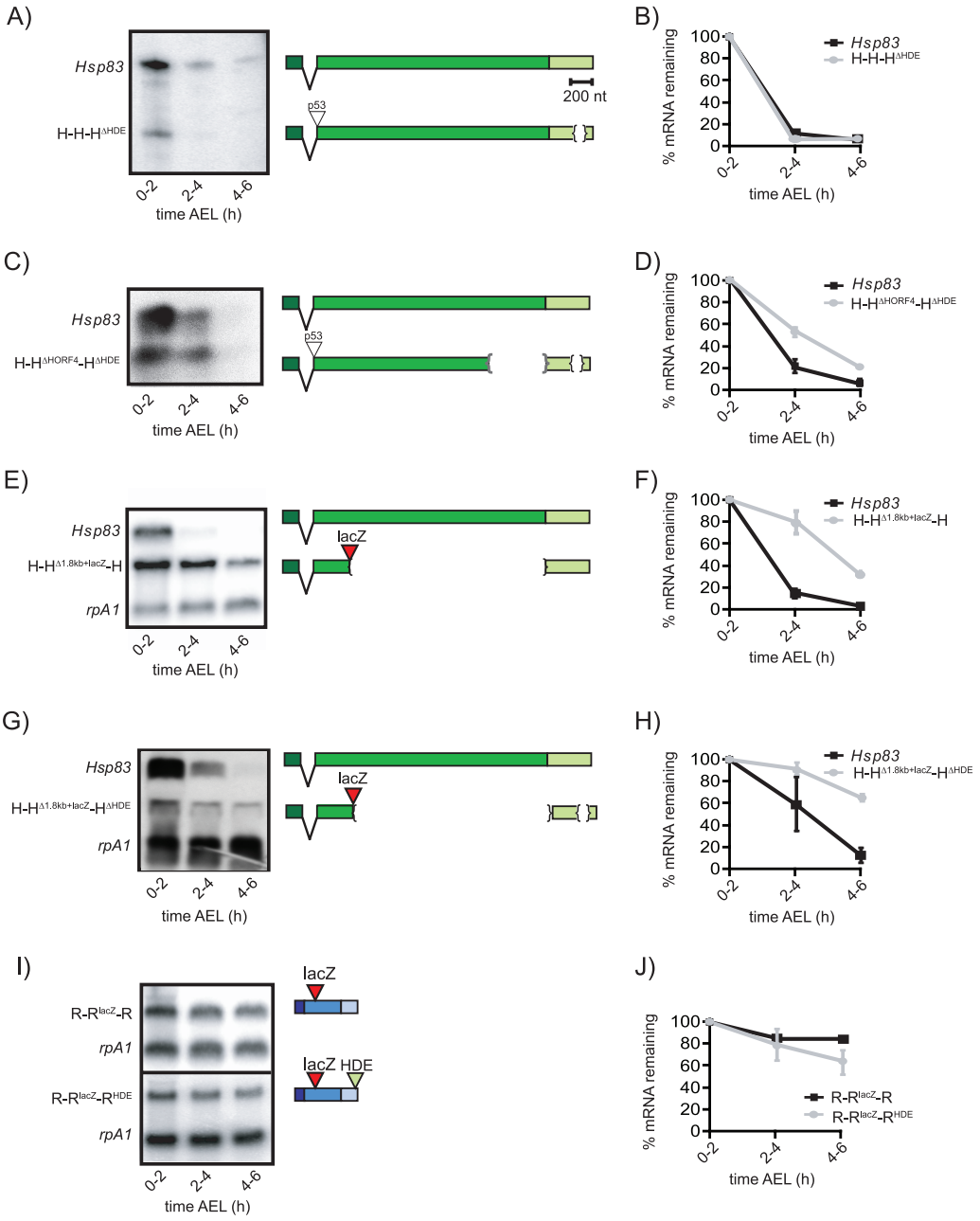

FIG. 4. Mapping of auxiliary ORF elements and the role of the HDE. (A and B) Test of the necessity of the HDE to mediate *Hsp83* mRNA decay via the maternal degradation pathway. (A) RNase H cleavage and Northern blot analysis of H-H-H$^{\Delta HDE}$ transgenic mRNA. *Hsp83* mRNA and H-H-H$^{\Delta HDE}$ mRNA were cleaved with RNase H in the presence of an oligonucleotide that anneals to the 3′ end of the ORF and oligo(dT), thus generating 407-nt and 307-nt 3′ UTR fragments without their poly(A) tails, respectively. The blot was probed with full-length *Hsp83* 3′ UTR. (B) Quantification of Northern blot data in panel B revealed similar degradation rates for *Hsp83* and H-H-H$^{\Delta HDE}$ transcripts. H-H-H$^{\Delta HDE}$ females were heterozygous for the H-H-H transgene, thus accounting for the differences in initial levels relative to *Hsp83* mRNA. Raw mRNA levels are shown. Experiments were performed in duplicate. (C and D) Deletion of the both the HIE and HDE does not stabilize *Hsp83* transcripts. Northern blots were probed with *Hsp83* probe, thus detecting both endogenous *Hsp83* transcripts and the transgenic RNA (C). Quantification (D) included normalization relative to *rpA1* transcripts. Experiments were performed in duplicate, and the averages ± standard deviations are shown. For H-H$^{\Delta HORF4}$-H, 22% ± 13% of transcripts remained at 4 to 6 h AEL while, for H-H$^{\Delta HORF4}$-H$^{\Delta HDE}$, 21% ± 0% remained at 4 to 6 h AEL compared with <10% of endogenous mRNA. (E and F) Deletion of a ~1.8-kb 3′ region of the *Hsp83* ORF weakly stabilizes the transcript. The H-H$^{\Delta 1.8kb+lacZ}$-H transgene contains a ~1.8-kb 3′ deletion of the *Hsp83* coding sequence (including deletion of the entire HIE) along with a 603-nt *lacZ* ORF substitution. No p53 tag was present. For the Northern blot analysis of H-H$^{\Delta 1.8kb+lacZ}$-H mRNA in unfertilized eggs, both endogenous *Hsp83* and H-H$^{\Delta 1.8kb+lacZ}$-H mRNAs were detected by probing for *Hsp83*. *rpA1* mRNA was used as a loading control. Quantification values are the averages of three independent replicates for H-H$^{\Delta 1.8kb+lacZ}$-H. (G and H) Role of the HDE is revealed in a sensitized background. Northern blots were probed with *Hsp83* probe, thus detecting both endogenous *Hsp83* transcripts and the transgenic RNA. Quantification (H) included normalization relative to *rpA1* transcripts. Experiments were performed in duplicate, and the averages ± standard deviations are shown. For H-H$^{\Delta 1.8kb+lacZ}$-H, 31% ± 3% of transcripts remained at 4 to 6 h AEL (F) while, for H-H$^{\Delta 1.8kb+lacZ}$-H$^{\Delta HDE}$, 66% ± 3.7% remained at 4 to 6 h AEL (H). (I and J) Sufficiency of the HDE. R-R^{lacZ}-R and R-R^{lacZ}-R^{HDE} were derived from the same genomic *rpA1* DNA as R-R-R but lacked the p53 epitope tag and restriction sites at the 5′-UTR/ORF and ORF/3′-UTR junctions. Instead, these constructs contained a *lacZ* tag within their coding sequence. For Northern blot analysis of transgenic R-R^{lacZ}-R and R-R^{lacZ}-R^{HDE} mRNA, blots were probed with full-length *rpA1* to detect both endogenous and transgenic mRNAs. For quantification of Northern blot data of R-R^{lacZ}-R and R-R^{lacZ}-R^{HDE}, experiments were replicated two and five times, respectively, and the averages of those experiments ± standard deviations are shown. Constructs are drawn to scale.

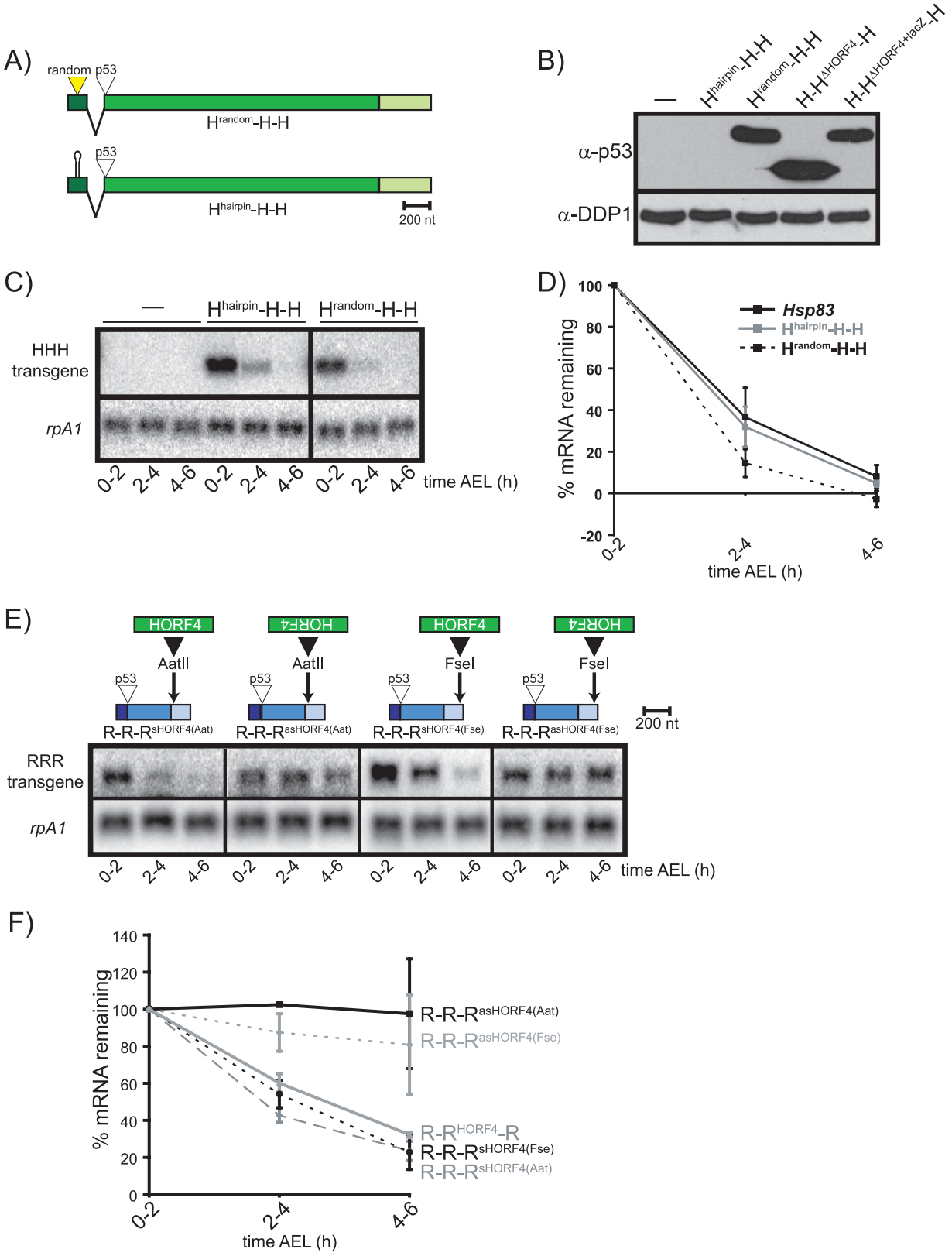

FIG. 5. *Hsp83* mRNA destabilization does not require translation in *cis*. (A to D) Insertion of a strong stable hairpin into full-length *Hsp83* transgenic mRNA blocks translation in *cis* but does not prevent mRNA degradation. (A) Schematic representation of the insertion of either a strong stable hairpin or random nonhairpin sequence (inverted triangle) into the 5′ UTR of H-H-H. Constructs are drawn to scale. (B) Western blot analysis using anti-p53 antibody demonstrates that protein was not detectable from 0- to 2-h unfertilized egg collections from $H^{hairpin}$-H-H transgenic mothers in contrast to H^{random}-H-H transgenic mothers. Specificity of the anti-p53 antibody and the proper sizes of the p53-tagged

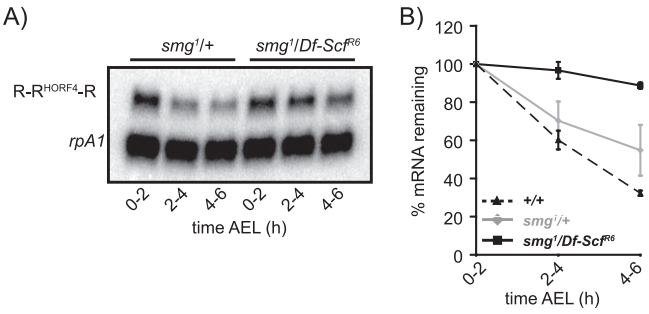

FIG. 6. SMG is required for the destabilization of R-R^{HORF4}-R transgenic mRNA. (A) Northern blot analysis of R-R^{HORF4}-R mRNA as assayed in *smg*^{1} heterozygous and *smg* mutant backgrounds. *smg*^{1} heterozygous and *smg*^{1} mutant eggs were both derived from mothers containing a single copy of the R-R^{HORF4}-R transgene. *smg* mutant eggs were derived from females containing the *smg*^{1} allele and the deficiency *Df(3L)Scf*^{R6}, which uncovers the *smg* region. Blots were probed as previously described for Fig. 3. (B) Quantification of Northern blot data in panel A. Average normalized transgenic mRNA levels between two independently derived transgenic fly lines are shown. The decay profile of R-R^{HORF4}-R in a +/+ background was taken from Fig. 1C and is included as a reference. Egg collection time points were the same, and normalizations were performed, as described for Fig. 1 and in Materials and Methods.

(Fig. 5E and F). In contrast, control antisense HIE insertions caused only 2% ± 30% and 19% ± 27% of the mRNA to be eliminated, respectively, for R-R-R$^{asHORF4(Aat)}$ and R-R-R$^{asHORF4(Fse)}$ mRNAs. Thus, the HIE can mediate transcript degradation even when located in the 3′ UTR, and ribosome transit through the HIE is not necessary for its function.

We conclude that translation in *cis* of the *Hsp83* mRNA and, specifically, of the HIE is not necessary for transcript degradation and that the HIE mediates transcript decay in a position-independent manner.

The HIE mediates SMG-dependent mRNA degradation. We have shown previously that SMG function is required for destabilization of endogenous *Hsp83* mRNA (30). We therefore next assessed whether HIE-dependent destabilization depends on SMG function. To do so, we determined the degradation profiles of R-R^{HORF4}-R, R-R-R$^{sHORF4(Fse)}$, and R-R-R$^{asHORF4(Fse)}$ transgenic mRNA in unfertilized eggs produced by *smg* mutant females.

The degradation of R-R^{HORF4}-R and R-R-R$^{sHORF4(Fse)}$ mRNA was severely compromised—in a dose-dependent manner—by loss of SMG (Fig. 6 shows R-R^{HORF4}-R). In an *smg*^{1} heterozygous background (i.e., in the presence of one dose of the *smg*$^{+}$ gene), R-R^{HORF4}-R mRNA was partially stabilized relative to the wild type (55% ± 13% versus 32% ± 1%, respectively, remaining by 4 to 6 h AEL in unfertilized eggs). In an *smg*^{1} homozygous mutant background (i.e., zero doses of the *smg*$^{+}$ gene), transgenic R-R^{HORF4}-R mRNA was almost completely stabilized with 89% ± 2% of the mRNA remaining by 4 to 6 h AEL. This is almost identical to the stabilization of endogenous *Hsp83* mRNA in 2- to 3-h embryos from *smg* mutant females, in which 92% ± 4% of endogenous *Hsp83* transcripts remain (30). Likewise, R-R-R$^{sHORF4(Fse)}$ transcripts were stabilized in *smg*^{1} homozygotes (data not shown). We conclude that the HIE functions in an SMG-dependent manner, thus reflecting a true endogenous major instability element.

The HIE directs association with SMG protein. We previously used real-time RT-PCR to show that endogenous *Hsp83* transcripts are present in an SMG-containing messenger ribonucleoprotein complex (mRNP): after immunoprecipitation with anti-SMG antibody, *Hsp83* transcripts were fivefold enriched relative to normal rat serum; a positive control, *nanos*, was also fivefold enriched; and a negative control, *rp49*, was only 1.7-fold enriched (30). To assess whether the HIE is sufficient to target a hybrid mRNA to the SMG-containing mRNP, here we again used real-time RT-PCR to study the R-R^{HORF4}-R and R-R-R$^{sHORF4(Fse)}$ mRNAs. We found that the R-R^{HORF4}-R and R-R-R$^{sHORF4(Fse)}$ transcripts were enriched 3.3- ± 0.5-fold and 5.6- ± 1.2-fold, respectively, while endogenous *Hsp83* transcripts were enriched 5.6- ± 0.5-fold and 4.5- ± 0.3-fold and *rp49* transcripts were enriched 1.3- ± 0.0-fold and 1.6- ± 0.4-fold in their respective experiments.

We conclude that the HIE can direct transcripts into an SMG-containing mRNP.

SMG's RNA-binding ability is necessary for *Hsp83* mRNA destabilization. Alanine$_{498}$ of the budding yeast homolog of SMG, VTS1, is found in its RNA-binding domain (RBD) and makes direct contact with the third base in the loop of the SRE (1). A single amino acid mutation (to histidine) of either alanine$_{498}$ within the VTS1 SAM domain or the analogous residue within the SMG SAM domain, alanine$_{642}$, completely abolishes the ability of these SAM domains to bind consensus SREs in vitro but does not disrupt protein folding (2).

To assess whether direct binding of SMG to *Hsp83* mRNA is required for transcript destabilization, we therefore made full-length SMG "rescue" constructs expressing either wild-type protein (SMG^{WT}) or an A642H mutant protein (SMG^{RBD}, for RBD mutant). Using the modified GAL4/upstream activation

transgenic protein were demonstrated by looking at additional p53-tagged constructs such as H-H$^{\Delta HORF4}$-H and H-H$^{\Delta HORF4+lacZ}$-H. (C) Northern blot analysis of H^{hairpin}-H-H and H^{random}-H-H mRNA. Transgenic mRNAs were detected using a p53-specific probe, and *rpA1* mRNA was used as a loading control. Lanes marked "−" denote unfertilized eggs lacking any transgene. (D) Quantification of Northern blot data in panel C. Average normalized transgenic mRNA levels from two independently derived transgenic fly lines are shown. The endogenous *Hsp83* mRNA decay profile from Fig. 1 is included as a reference. Egg collection time points and normalization were as described for Fig. 1. (E and F) The HIE mediates the decay of stable *rpA1* transgenic mRNA in a position-independent but orientation-dependent manner. (E) The HIE was inserted in sense and antisense orientations at two different locations within the *rpA1* 3′ UTR (and thus downstream of the stop codon). Northern blot analysis of transgenic mRNAs in unfertilized eggs is shown below the schematic representations (drawn to scale). Blots were probed with the full-length *rpA1* 3′ UTR, which detected both transgenic (experimental) and *rpA1* (loading control) transcripts. (F) Quantification of Northern blot data in panel E. Average normalized transgenic mRNA levels from two independently derived transgenic fly lines are shown. Egg collection time points were the same, and normalizations were performed, as described in Materials and Methods. The decay profile of R-R^{HORF4}-R from Fig. 1C is included as a reference.

A)

	Rescue Construct		Driver	Genotype	
	pUASP-SMG^{WT}	pUASP-SMG^{RBD}	nosGAL4^{VP16}	*smg^1*/+	*smg^1*/*smg^1*
1	–	–	+	–	+
2	–	+	+	–	+
3	–	+	+	+	–
4	–	+	–	+	–
5	+	–	+	+	–
6	+	–	–	+	–
7	–	–	+	–	+
8	+	–	+	–	+

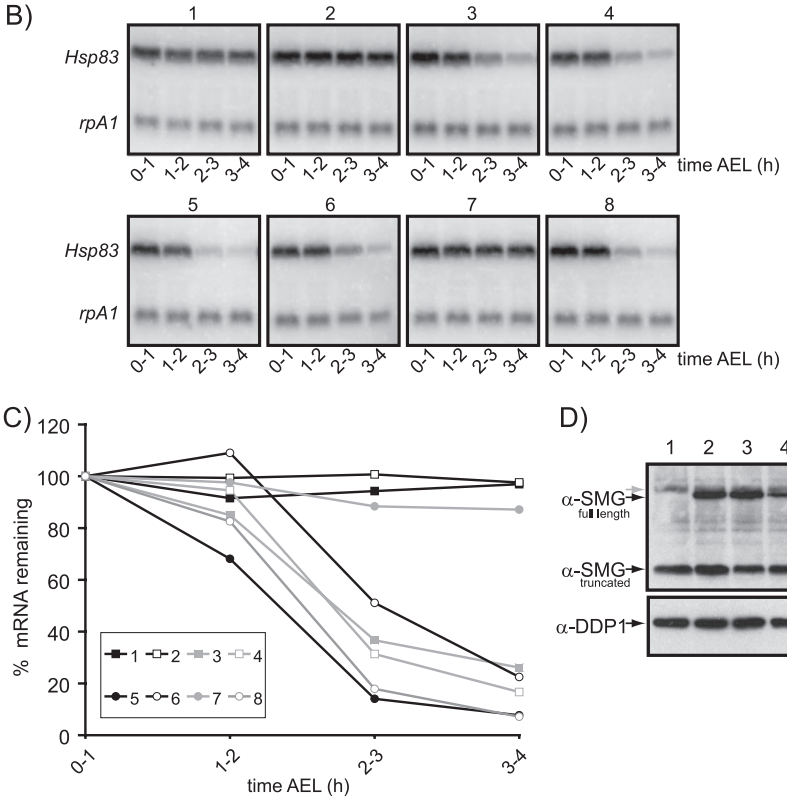

FIG. 7. RNA-binding ability of SMG is necessary for degradation of endogenous *Hsp83* mRNA. Full-length SMG transgenes driven by the GAL4/UAS system were tested for their ability to rescue the *Hsp83* mRNA degradation phenotype in *smg^1* mutant embryos. The function of the wild-type rescue construct (SMG^{WT}) was compared to that of a mutated SMG construct (SMG^{RBD}) which contains a single point mutation within the sequence encoding the SMG RBD, which is predicted to abolish SMG's ability to bind its cognate RNA sequence, the SRE. Rescue constructs were expressed using pUASP vectors and were driven via the maternal driver, nosGAL4^{VP16}. (A) Genetic background of transgenic mothers with sibling control lines included. (B) Northern blot analysis of total RNA extracted from fertilized embryos over a 4-hour time course. Embryos were examined at 0 to 1, 1 to 2, 2 to 3, and 3 to 4 h AEL. Blots were probed for *Hsp83* (experimental) and *rpA1* (loading control) mRNAs. Genotypes are described in the legend to panel A. (C) Quantification of Northern blot data in panel B. Only a single experiment was performed. Normalization was as described for Fig. 1. (D) Western blot analysis of 0- to 3-h embryos demonstrating the production of SMG protein from the rescue constructs SMG^{WT} and SMG^{RBD}. The anti-SMG antibody recognizes both the endogenous and the transgenic SMG proteins, as well as the truncated form of the protein derived from the *smg^1* allele. Anti-DDP1 antibody was used as a loading control. The gray arrow represents a cross-reacting band that migrates just above the SMG protein.

sequence (UAS) system to drive expression of the transgenic mRNAs during oogenesis (27, 41), we assessed the ability of SMG^{RBD} and SMG^{WT} to rescue the severe *Hsp83* mRNA degradation defects observed in *smg* mutants. In these experiments, because we had shown that *Hsp83* mRNA degradation is SMG dependent in both unfertilized and fertilized eggs (30) and the amount of material was limiting, embryos rather than unfertilized eggs were used.

Expression of SMG^{WT} in embryos from *smg* mutant females fully rescued endogenous *Hsp83* mRNA destabilization (Fig. 7A to C, genotype 8). In sibling controls, *Hsp83* mRNA decay was observed in *smg^1* heterozygous backgrounds (Fig. 7A to C, genotypes 5 and 6), while *Hsp83* mRNA was completely stabilized in embryos from *smg^1* mutant mothers lacking the SMG^{WT} transgene (Fig. 7A to C, genotype 7). In striking contrast, embryos expressing SMG^{RBD} failed to degrade endogenous *Hsp83* mRNA (Fig. 7A to C, genotype 2); this decay profile was indistinguishable from that observed in the *smg^1* mutant background alone (Fig. 7A to C, genotype 1). Embryos from their *smg^1* heterozygous siblings, in contrast,

displayed normal *Hsp83* mRNA decay (Fig. 7A to C, genotypes 3 and 4).

Western blot analysis confirmed that pUASP-SMG^{WT} and pUASP-SMG^{RBD} produced equivalent levels of SMG protein (Fig. 7D); therefore, the lack of rescue by SMG^{RBD} was not attributable to lower protein levels. The results shown in Fig. 7 derive from single transgenic lines for SMG^{WT} and SMG^{RBD}; almost-identical results were obtained for two additional transgenic lines for each construct (data not shown). Thus, a point mutation that abrogates the SRE binding ability of SMG also blocks the ability of SMG to mediate *Hsp83* mRNA destabilization, consistent with direct binding of SMG to the *Hsp83* mRNA being a prerequisite for transcript destabilization.

Simultaneous mutation of all eight computationally predicted SREs in the *Hsp83* ORF stabilizes the transcript. SMG recognizes its target mRNAs via stem-loop structures called SREs (12, 32, 33). Initially, the consensus SRE sequence was defined as either a 4- or a 5-nt loop with the sequence CNGG or CNGGN, respectively, on a nonspecific stem (2, 11). Four copies of this consensus SRE, present within the ORF of endogenous *Hsp83* mRNA, were shown by us to be dispensable since simultaneous mutation of all four elements did not affect transcript instability (30). Subsequent to those analyses, it was shown that the length of an SRE loop can be increased to 7 nt ($CNGGN_{0–3}$) and the SRE can remain fully functional (1). In addition, structural analyses revealed that the VTS1 RBD makes contact with the phosphate groups between the third and fourth bases of the stem, suggesting that the length of the stem may also be important for RNA recognition (1). A computational search of the entire *Hsp83* transcript for the revised SRE consensus ($CNGGN_{0–3}$ on a stem of at least 4 bp) revealed an additional four predicted SREs within the *Hsp83* mRNA. Thus, there are a total of eight predicted SREs in the *Hsp83* mRNA: all map within the ORF, six of the eight reside within the HIE, and seven of the eight are removed by the 1.8-kb deletion used in our analyses reported above (in Fig. 9 the four potential SREs that were mutated in our 2005 study are indicated with asterisks; see also Fig. S1 in the supplemental material for the complete sequence of the ORF and location of the SREs).

To assess whether destabilization of *Hsp83* mRNA requires binding to these predicted SREs, we constructed a transgene encoding an mRNA—H-H$^{8xSRE(-)}$-H—in which all eight sites were mutated simultaneously (Fig. 8; see also Fig. S1 in the supplemental material). In seven out of eight cases, third-base mutations ensured that the transgene retained identical amino acid coding capacity; in one case it was necessary to introduce a conservative substitution (see Materials and Methods and Fig. S1 in the supplemental material).

Northern blot analysis of H-H$^{8xSRE(-)}$-H mRNA showed that it was strongly stabilized: by 4 to 6 h AEL in unfertilized eggs 76% ± 27% of transgenic transcripts remained, compared with only 13% ± 4% of endogenous *Hsp83* transcripts in controls (Fig. 8). Strong stabilization also occurred in embryos, with 68% ± 12% of the H-H$^{8xSRE(-)}$-H transcripts remaining at 3 to 4 h AEL (data not shown).

Together with our results obtained by point mutation of SMG's RBD, we conclude that SMG interacts directly with the SREs in the *Hsp83* ORF to destabilize the mRNA. Since mutation of four out of the eight predicted SREs did not abrogate transcript destabilization (30) while mutation of all eight did, we conclude that SMG is likely to bind to more than four SREs to destabilize the *Hsp83* transcript.

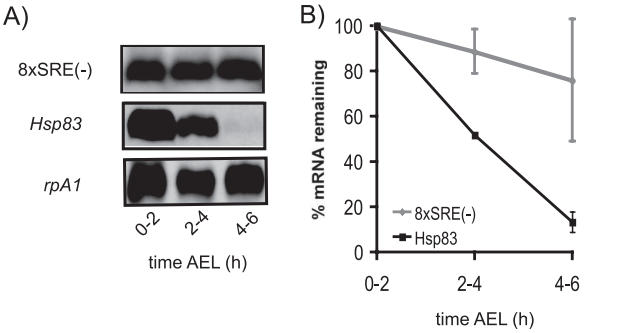

FIG. 8. Mutation of eight predicted SREs in the *Hsp83* ORF results in transcript stabilization. (A) Northern blot analysis of H-H$^{8xSRE(-)}$-H transcripts [8xSRE(-)] and endogenous *Hsp83* mRNAs in unfertilized eggs. H-H$^{8xSRE(-)}$-H transcripts were detected by probing with the p53-LNA-3′-digoxigenin probe described in Materials and Methods. Endogenous *Hsp83* mRNA from non-8xSRE(-) eggs served as a positive control for instability, and endogenous *rpA1* mRNA was used as a loading control for normalization. H-H$^{8xSRE(-)}$-H transcripts were strongly stabilized: by 4 to 6 h AEL in unfertilized eggs, 76% ± 27% of transgenic transcripts were present compared with only 13% ± 4% of endogenous *Hsp83* transcripts. (B) Quantification of Northern blot data in panel A. Error bars represent standard deviations calculated from at least two independent experiments.

DISCUSSION

We have shown here that the *Drosophila Hsp83* mRNA contains one major and several minor instability elements that direct transcript degradation upon egg activation via what we previously termed the "maternal degradation pathway" (4). The major instability element (the HIE) resides in the 3′-most 615 nt of the ORF but does not require ribosome transit for its destabilizing function. The HIE contains six of the eight predicted SREs in the *Hsp83* transcript and is able to direct an mRNA to associate with an SMG-containing mRNP, thus conferring SMG-dependent destabilization on that transcript. Two additional predicted SREs are present outside the HIE, in the more-5′ part of the *Hsp83* ORF. Mutation of the SMG RBD or of all eight SREs results in stabilization of the *Hsp83* transcript. Thus, SMG directly interacts with multiple SREs in the *Hsp83* ORF to recruit the CCR4-NOT deadenylase and trigger decay. The only previously identified *Drosophila* transcript shown to be directly bound by SMG is *nanos*, which has two SREs in its 3′ UTR (11, 12, 32, 33). However, precedent for an ORF-located SRE comes from budding yeast, where it has been shown that the ORF of the *NNF1* mRNA contains a single SRE, which confers VTS1-dependent instability (1).

Our analyses have also shown that an auxiliary instability element (the HDE [4]) resides in the *Hsp83* 3′ UTR. The HDE is capable of weakly destabilizing an otherwise stable mRNA (*rpA1*); however, its role in the context of the *Hsp83* mRNA is revealed only in a situation in which more than 80% of the ORF is deleted—including seven of the eight predicted SREs—thus partially stabilizing the transcript and sensitizing it to deletion of the HDE.

Mechanism of HIE function. Studies of c-*fos* and c-*myc* mRNA decay in mammalian cells and *MATα1* mRNA decay in *S. cerevisiae* have provided a detailed mechanistic understanding of how coding region determinants (CRDs) act to destabilize their mRNAs (7–9, 18, 22, 29). The rapid decay of c-*fos* mRNA involves the formation of a pre-translation-initiation mRNP that acts to bridge the coding region instability element with the poly(A) tail via the RNA-binding proteins UNR, PABP, PAIP, hnRNP D, and NSAP. Upon ribosome transit, mRNP reorganization permits access of the CCR4-NOT deadenylase to the poly(A) tail, leading to mRNA degradation. In contrast, degradation of c-*myc* and *MATα1* mRNAs is due to ribosome pausing at rare codons found in the vicinity of the CRDs. It is believed that ribosome stalling creates a downstream region devoid of ribosomes, which can be accessed by the degradation machinery unless the regions downstream of the rare codons are bound by protective RNA-binding factors.

Translation-independent CRDs, which function either to stabilize or to destabilize mRNAs, have been identified in several transcripts. Stabilizing elements reside in the ORF of the yeast *OLE1* mRNA (42), and destabilizing elements map to the ORFs of mammalian *PAI-2* and *MnSOD* mRNAs (14, 40). The CRDs in *PAI-2* and *MnSOD* mRNAs do not require ribosome transit and function when inserted into a 3′ UTR. *trans*-acting RNA-binding proteins required for the function of the CRDs of *PAI-2* and *MnSOD* have yet to be identified, and their decay mechanisms remain unknown.

Formally, the HIE resembles the *PAI-2* and *MnSOD* CRDs. Maternally loaded *Hsp83* mRNA is actively translated in the early *Drosophila* embryo (30), and we have shown here that a 5′ UTR hairpin that inhibits translation has no effect on *Hsp83* transcript instability. Despite the fact that the HIE maps within the coding region, it continues to function when inserted into a 3′ UTR. Thus, ribosome transit is not required for HIE function. Below we present a model for the role of the HIE—and its resident SREs—in transcript destabilization.

The role of the HDE. Our previous work identified the 97-nt HDE in the *Hsp83* 3′ UTR as an instability element that functions in the maternal degradation pathway (3, 4). We have shown here that these earlier results were a consequence of the use of a reporter mRNA (H-H$^{\Delta 1.8kb+lacZ}$-H) lacking most of the ORF-located instability elements (seven of eight SREs) and sensitized to deletion of the auxiliary element. Deletion of the HDE in this context (H-H$^{\Delta 1.8kb+lacZ}$-H$^{\Delta HDE}$) thus resulted in strong transcript stabilization while the same reporter without the HDE deletion was only weakly unstable.

Our previous analyses also suggested that the HDE might function both as an instability element and as a translational enhancer (4). We have recently identified a multiprotein complex that binds the HDE and mediates translational enhancement (24). Three proteins—DDP1, HRP48, and PABP—function together to stimulate translation. To date, none of these proteins has been implicated in the transcript destabilization function of the HDE.

SMG, SREs, and *Hsp83* mRNA destabilization. In a previous study we identified and simultaneously mutated four potential SREs in the *Hsp83* ORF without affecting transcript destabilization (30). Identification of those SREs was based on the loop consensus CNGGN$_{0-1}$ (2). More recently, a revised loop consensus sequence (CNGGN$_{0-3}$) (1) enabled us to identify four additional predicted SREs within the *Hsp83* transcript. Thus, there are a total of eight predicted SREs in the *Hsp83* mRNA, all in the ORF (Fig. 9; see also Fig. S1 in the supplemental material). Of the large fragments of the ORF that were tested for sufficiency, only HORF4 (the HIE) was able to confer strong instability, and it contains six of the predicted SREs. The other three large fragments (HORF1, HORF2, and HORF3) each contain a single predicted SRE and did not, by themselves, confer instability. Of the subfragments of HORF4 that were sufficient to confer weak instability, two contain three predicted SREs (HORF4-7 and HORF4-8), one contains two predicted SREs (HORF4-1), and one (HORF4-6) carries a single predicted SRE. In contrast, of the four subfragments of ORF4 that were not sufficient to confer instability, three contain a single predicted SRE (HORF4-3, HORF4-4, and HORF4-5) and one (HORF4-2) contains no predicted SRE. Thus, there is a good correlation between the number of predicted SREs in a fragment and its ability to destabilize a hybrid mRNA. Based on this correlation, a plausible hypothesis is that multiple SREs in the *Hsp83* mRNA's ORF function together to bind strongly to SMG and recruit the transcript to an SMG-containing mRNP, following which deadenylation by the CCR4-NOT deadenylase triggers decay.

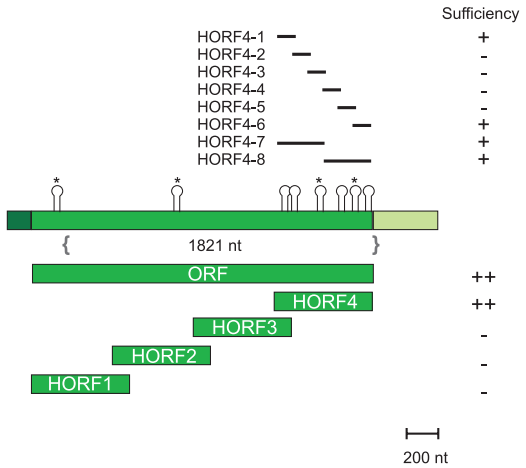

FIG. 9. Potential SREs in the *Hsp83* mRNA and their relationships to fragments of the ORF that are sufficient to destabilize the *rpA1* transcript. The diagrams and color coding are as in Fig. 1 to 4. Predicted SREs (defined as in the text) are shown at their approximate locations in the *Hsp83* mRNA but are drawn larger than scale. Asterisks indicate the predicted SREs that were mutated in our previous study (30). The braces indicate the 1,821-nt deletion that incompletely abrogates instability of the *Hsp83* transcript. The ability of the full-length ORF and its subfragments to confer instability as defined in Table 1 is indicated to the right: ++, strong instability element; +, moderate instability element; −, no destabilizing activity.

Two complementary approaches were used to prove that SMG binding to multiple SREs in the *Hsp83* ORF is required to trigger destabilization. First, a single-amino-acid substitution, A462H, in the RBD of SMG completely stabilized the endogenous *Hsp83* mRNA. Second, simultaneous mutation of all eight predicted SREs (without significantly affecting the coding capacity of the ORF) stabilized a transgenic *Hsp83* transcript.

The fact that mutation of four of the predicted SREs (two in

the HIE) did not stabilize the mRNA (30) whereas mutation of all eight predicted SREs (six in the HIE) did suggests a requirement for multiple SREs in *Hsp83* transcript destabilization. Using metabolic labeling with [^{35}S]methionine, we showed previously that, in early embryos, *Hsp83* transcripts are in fact translated as well as destabilized (30). In light of this fact, the location of all of the predicted SREs in the *Hsp83* ORF rather than its UTRs has mechanistic implications for transcript destabilization since SMG cannot remain bound while a ribosome transits through an SRE. First, it is possible that only a fraction of *Hsp83* mRNA is translated in early embryos; thus, most of the maternal *Hsp83* transcripts may exist in an untranslated state with SMG bound and, therefore, able to recruit the deadenylase. Alternatively, most *Hsp83* transcripts may be translated and their destabilization may result from the distribution of multiple SREs over a large domain rather than clustered as a pair as in the 3′ UTR of the *nanos* mRNA (11, 12, 32, 33). A plausible model is that multiple, widely spaced SREs ensure that some SMG molecules remain bound to an *Hsp83* mRNA molecule even as ribosomes transit its ORF. The *Hsp83* mRNA could, then, be targeted for deadenylation and decay even though it was simultaneously being translated. Thus, the SREs in the ORF permit transcript destabilization in spite of—but not because of—translation.

ACKNOWLEDGMENTS

We thank Arash Bashirullah for designing and Tyler Davies for making the H-H-H$^{\Delta HDE}$ construct. Najeeb Siddiqui and Wael Tadros kindly provided critical comments on a draft of the manuscript.

Trainee support came from the following sources: a Natural Sciences and Engineering Research Council of Canada (NSERC) Graduate Scholarship (J.L.S.), a Canada Graduate Scholarship from the Canadian Institutes for Health Research (CIHR) (J.L.S.), studentships from the Ontario Student Opportunity Trust-Hospital for Sick Children Foundation Student Scholarship Program (J.L.S. and R.L.C.), and a scholarship from the CIHR (R.L.C.). H.D.L. is Canada Research Chair (Tier 1) in Developmental Biology at the University of Toronto. This research was supported by an operating grant to C.A.S. from the National Cancer Institute of Canada with funds from the Terry Fox Run and an operating grant (MOP-14409) to H.D.L. from the CIHR.

REFERENCES

1. **Aviv, T., Z. Lin, G. Ben-Ari, C. A. Smibert, and F. Sicheri.** 2006. Sequence-specific recognition of RNA hairpins by the SAM domain of Vts1p. Nat. Struct. Mol. Biol. **13:**168–176.
2. **Aviv, T., Z. Lin, S. Lau, L. M. Rendl, F. Sicheri, and C. A. Smibert.** 2003. The RNA-binding SAM domain of Smaug defines a new family of post-transcriptional regulators. Nat. Struct. Biol. **10:**614–621.
3. **Bashirullah, A., R. L. Cooperstock, and H. D. Lipshitz.** 2001. Spatial and temporal control of RNA stability. Proc. Natl. Acad. Sci. USA **98:**7025–7028.
4. **Bashirullah, A., S. R. Halsell, R. L. Cooperstock, M. Kloc, A. Karaiskakis, W. W. Fisher, W. Fu, J. K. Hamilton, L. D. Etkin, and H. D. Lipshitz.** 1999. Joint action of two RNA degradation pathways controls the timing of maternal transcript elimination at the midblastula transition in Drosophila melanogaster. EMBO J. **18:**2610–2620.
5. **Bettegowda, A., and G. W. Smith.** 2007. Mechanisms of maternal mRNA regulation: implications for mammalian early embryonic development. Front. Biosci. **12:**3713–3726.
6. **Blackman, R. K., and M. Meselson.** 1986. Interspecific nucleotide sequence comparisons used to identify regulatory and structural features of the Drosophila hsp82 gene. J. Mol. Biol. **188:**499–515.
7. **Caponigro, G., D. Muhlrad, and R. Parker.** 1993. A small segment of the *MAT*α*1* transcript promotes mRNA decay in *Saccharomyces cerevisiae*: a stimulatory role for rare codons. Mol. Cell. Biol. **13:**5141–5148.
8. **Caponigro, G., and R. Parker.** 1996. mRNA turnover in yeast promoted by the MATalpha1 instability element. Nucleic Acids Res. **24:**4304–4312.
9. **Chang, T. C., A. Yamashita, C. Y. Chen, Y. Yamashita, W. Zhu, S. Durdan, A. Kahvejian, N. Sonenberg, and A. B. Shyu.** 2004. UNR, a new partner of poly(A)-binding protein, plays a key role in translationally coupled mRNA turnover mediated by the c-fos major coding-region determinant. Genes Dev. **18:**2010–2023.
10. **Cooperstock, R. L.** 2002. Mechanisms of transcript regulation in the early Drosophila embryo: degradation, localization and translational regulation. Ph.D. thesis. University of Toronto, Toronto, Ontario, Canada.
11. **Crucs, S., S. Chatterjee, and E. R. Gavis.** 2000. Overlapping but distinct RNA elements control repression and activation of nanos translation. Mol. Cell **5:**457–467.
12. **Dahanukar, A., J. A. Walker, and R. P. Wharton.** 1999. Smaug, a novel RNA-binding protein that operates a translational switch in Drosophila. Mol. Cell **4:**209–218.
13. **Dahanukar, A., and R. P. Wharton.** 1996. The Nanos gradient in Drosophila embryos is generated by translational regulation. Genes Dev. **10:**2610–2620.
14. **Davis, C. A., J. M. Monnier, and H. S. Nick.** 2001. A coding region determinant of instability regulates levels of manganese superoxide dismutase mRNA. J. Biol. Chem. **276:**37317–37326.
15. **Decker, C. J., and R. Parker.** 1993. A turnover pathway for both stable and unstable mRNAs in yeast: evidence for a requirement for deadenylation. Genes Dev. **7:**1632–1643.
16. **De Renzis, S., O. Elemento, S. Tavazoie, and E. F. Wieschaus.** 2007. Unmasking activation of the zygotic genome using chromosomal deletions in the Drosophila embryo. PLoS Biol. **5:**e117.
17. **Fontes, A. M., A. Riedl, and M. Jacobs-Lorena.** 2001. Developmental regulation of an instability element from the Drosophila fushi tarazu mRNA. Genesis **30:**59–64.
18. **Grosset, C., C. Y. Chen, N. Xu, N. Sonenberg, H. Jacquemin-Sablon, and A. B. Shyu.** 2000. A mechanism for translationally coupled mRNA turnover: interaction between the poly(A) tail and a c-fos RNA coding determinant via a protein complex. Cell **103:**29–40.
19. **Ito, J., and M. Jacobs-Lorena.** 2001. Functional mapping of destabilizing elements in the protein-coding region of the Drosophila fushi tarazu mRNA. J. Biol. Chem. **276:**23525–23530.
20. **Kozak, M.** 1989. Circumstances and mechanisms of inhibition of translation by secondary structure in eucaryotic mRNAs. Mol. Cell. Biol. **9:**5134–5142.
21. **Lecuyer, E., H. Yoshida, N. Parthasarathy, C. Alm, T. Babak, T. Cerovina, T. R. Hughes, P. Tomancak, and H. M. Krause.** 2007. Global analysis of mRNA localization reveals a prominent role in organizing cellular architecture and function. Cell **131:**174–187.
22. **Lemm, I., and J. Ross.** 2002. Regulation of c-*myc* mRNA decay by translational pausing in a coding region instability determinant. Mol. Cell. Biol. **22:**3959–3969.
23. **Lipshitz, H. D., and C. A. Smibert.** 2000. Mechanisms of RNA localization and translational regulation. Curr. Opin. Genet. Dev. **10:**476–488.
24. **Nelson, M. R., H. Luo, H. K. Vari, B. J. Cox, A. J. Simmonds, H. M. Krause, H. D. Lipshitz, and C. A. Smibert.** 2007. A multiprotein complex that mediates translational enhancement in Drosophila. J. Biol. Chem. **282:**34031–34038.
25. **Richter, J. D.** 2007. CPEB: a life in translation. Trends Biochem. Sci. **32:**279–285.
26. **Riedl, A., and M. Jacobs-Lorena.** 1996. Determinants of *Drosophila fushi tarazu* mRNA instability. Mol. Cell. Biol. **16:**3047–3053.
27. **Rorth, P.** 1998. Gal4 in the Drosophila female germline. Mech. Dev. **78:**113–118.
28. **Rubin, G. M., and A. C. Spradling.** 1982. Genetic transformation of Drosophila with transposable element vectors. Science **218:**348–353.
29. **Schiavi, S. C., C. L. Wellington, A. B. Shyu, C. Y. Chen, M. E. Greenberg, and J. G. Belasco.** 1994. Multiple elements in the c-fos protein-coding region facilitate mRNA deadenylation and decay by a mechanism coupled to translation. J. Biol. Chem. **269:**3441–3448.
30. **Semotok, J. L., R. L. Cooperstock, B. D. Pinder, H. K. Vari, H. D. Lipshitz, and C. A. Smibert.** 2005. Smaug recruits the CCR4/POP2/NOT deadenylase complex to trigger maternal transcript localization in the early Drosophila embryo. Curr. Biol. **15:**284–294.
31. **Semotok, J. L., and H. D. Lipshitz.** 2007. Regulation and function of maternal mRNA destabilization during early Drosophila development. Differentiation **75:**482–506.
32. **Smibert, C. A., Y. S. Lie, W. Shillinglaw, W. J. Henzel, and P. M. Macdonald.** 1999. Smaug, a novel and conserved protein, contributes to repression of nanos mRNA translation in vitro. RNA **5:**1535–1547.
33. **Smibert, C. A., J. E. Wilson, K. Kerr, and P. M. Macdonald.** 1996. smaug protein represses translation of unlocalized nanos mRNA in the Drosophila embryo. Genes Dev. **10:**2600–2609.
34. **Surdej, P., and M. Jacobs-Lorena.** 1998. Developmental regulation of *bicoid* mRNA stability is mediated by the first 43 nucleotides of the 3′ untranslated region. Mol. Cell. Biol. **18:**2892–2900.
35. **Tadros, W., A. L. Goldman, T. Babak, F. Menzies, L. Vardy, T. Orr-Weaver, T. R. Hughes, J. T. Westwood, C. A. Smibert, and H. D. Lipshitz.** 2007. SMAUG is a major regulator of maternal mRNA destabilization in Drosophila and its translation is activated by the PAN GU kinase. Dev. Cell **12:**143–155.
36. **Tadros, W., S. A. Houston, A. Bashirullah, R. L. Cooperstock, J. L.**

Semotok, B. H. Reed, and H. D. Lipshitz. 2003. Regulation of maternal transcript destabilization during egg activation in Drosophila. Genetics **164:**989–1001.
37. **Tadros, W., and H. D. Lipshitz.** 2005. Setting the stage for development: mRNA translation and stability during oocyte maturation and egg activation in Drosophila. Dev. Dyn. **232:**593–608.
38. **Tadros, W., J. T. Westwood, and H. D. Lipshitz.** 2007. The mother-to-child transition. Dev. Cell **12:**847–849.
39. **Thummel, C. S., and V. Pirrotta.** 1991. New pCaSpeR P element vectors. Drosophila Info. Newsl. **2:**19.
40. **Tierney, M. J., and R. L. Medcalf.** 2001. Plasminogen activator inhibitor type 2 contains mRNA instability elements within exon 4 of the coding region. Sequence homology to coding region instability determinants in other mRNAs. J. Biol. Chem. **276:**13675–13684.
41. **Van Doren, M., A. L. Williamson, and R. Lehmann.** 1998. Regulation of zygotic gene expression in Drosophila primordial germ cells. Curr. Biol. **8:**243–246.
42. **Vemula, M., P. Kandasamy, C. S. Oh, R. Chellappa, C. I. Gonzalez, and C. E. Martin.** 2003. Maintenance and regulation of mRNA stability of the Saccharomyces cerevisiae OLE1 gene requires multiple elements within the transcript that act through translation-independent mechanisms. J. Biol. Chem. **278:**45269–45279.